TRANSIENT RESPONSE OF UNIFORM BEAMS

Thesis by

Roger Alan Anderson

In Partial Fulfillment of the Requirements

for the Degree of

Doctor of Philosophy

California Institute of Technology

1953

ACKNOWLEDGEMENTS

The author wishes to express his sincere appreciation to Professor Donald E. Hudson who directed this research and whose aid and encouragement made this work possible. The assistance of Professor George W. Housner, who read the manuscript and contributed valuable suggestions, is also acknowledged with thanks.

TABLE OF CONTENTS

ABSTRACT

Several special topics relating to the transient flexural vibrations of a uniform beam predicted by the usual elementary or Bernoulli-Euler equation are discussed. The effect on the beam response of the concentration of an applied transient force in space and in time is studied. In the case of an applied step force, it is shown that the dynamic beam response can be larger than twice the response to an equal force statically applied. It is demonstrated that the beam response in the higher modes is independent of the boundary conditions.

A new, general series solution of the mode superposition type is given for the flexural vibrations of a uniform beam according to the more refined Timoshenko equations including the secondary effects of shear deflections and rotatory inertia. As a special case, the solution is presented for a pin-ended beam. These solutions are characterized by two series, each of the form of the series solution of the Bernoulli-Euler equation.

For the special case of a concentrated transient force applied at the midpoint of a pin-ended beam, the bending moment and shear force solutions for the Timoshenko and Bernoulli-Euler equations are compared.

INTRODUCTION

In recent years, the subject of the transient vibrations of elastic structures has become important in engineering. This is particularly true of the problem of the transient flexural vibrations of elastic beams. The study of beam response is important because the beam is one of the most common structural elements and because it is one of the simplest continuous elastic structures. A study of its behavior will yield insight into the transient behavior of more complex structures.

The analytical determination of the transient flexural vibrations of beamsusually employs the Bernoulli-Euler or elementary equation of motion. This equation considers only the lateral inertia and the elastic forces due to bending deflections. However, it is known that secondary effects such as shear deflections and rotatory inertia which are not included in the Bernoulli-Euler equation may profoundly affect the flexural vibrational response under certain conditions.

The first and best known equation including the secondary effects of shear deflections and rotatory inertia is that of Timoshenko. The only correct solution of the Timoshenko equation that has been presented to date is that of Dengler and Goland who obtained, with the aid of Laplace and Fourier transforms, a flexural wave solution for a uniform, infinite beam subjected to a transverse impulse. No correct analytical solutions have been presented for finite beams. No analytical solutions in the series or mode superposition form

have been given. The bulk of the papers considering the Timoshenko theory have concentrated on the effect of shear deflections and rotatory inertia on the natural frequencies or on the velocities of propagation of elastic waves.

It is evident that solutions for the flexural response of a beam according to the Timoshenko equation are difficult to obtain and evaluate. Thus it is advantageous to apply the Bernoulli-Euler equation whenever possible. It is important then to determine the veracity of the Bernoulli-Euler equation under various conditions as compared with the Timoshenko equation and to define its region of usefulness. It is desirable to have a general solution of the Timoshenko equation to be applied outside the range of utility of the Bernoulli-Euler equation.

The series or mode superposition form of the solution of the Bernoulli-Euler equation has been universally found to be convenient for routine engineering calculations. It is believed that the same benefits will accrue to the mode superposition solution of the Timoshenko equation. For this reason, and since a comparison is to be made with the mode superposition solution of the Bernoulli-Euler equation, it was decided to attempt to derive a general mode superposition solution of the Timoshenko equation. The absence in this thesis of the flexural wave type solution is not meant to deny the importance of this type of solution.

This thesis presents the general solution in series or mode superposition for the flexural response of a uniform beam described

by the Timoshenko equations. Instead of the usual single Timoshenko equation in one variable, two simultaneous equations in two variables are treated. This results in a simpler statement of end conditions and simpler expressions for the elastic bending moment and shear force. An orthogonality condition is found which permits a solution. In addition to the general solution, the solution for the flexural vibrations in a uniform, pin-ended beam is presented. For the special case of a uniform, pin-ended beam subjected to a transient concentrated force at the midpoint, the elastic bending moments and shear forces are calculated and a comparison is made of the Bernoulli-Euler and Timoshenko solutions.

Although well known, the general solution of the Bernoulli-Euler equation is presented for convenience and for comparison with the solution of the Timoshenko equations. Several special topics of importance in the application of the Bernoulli-Euler equation are discussed.

I. BERNOULLI-EULER THEORY.

1. Solution by Superposition of Normal Modes.

This form of the solution can also be referred to as the solution in terms of standing waves or as the solution by means of separation of variables.

According to the well known Bernoulli-Euler theory, the vibrations of an undamped elastic beam are described by the equation (Ref. 1):

$$\frac{\partial^2}{\partial x^2}\left(EI\,\frac{\partial^2 y}{\partial x^2}\right) + \rho A\,\frac{\partial^2 y}{\partial t^2} = w\,(x,\,t). \qquad (1)$$

By way of review, this equation assumes that plane sections remain plane in bending and that the bending slopes are always small. The equation also requires that the line of centroids be a straight line, that the principal axes of the cross sections form two principal planes, and that the loading be applied in one of these principal planes. The equation neglects shear deflections and rotatory inertia forces. If the beam is uniform or prismatic, the equation of motion becomes:

$$EI\,\frac{\partial^4 y}{\partial x^4} + \rho A\,\frac{\partial^2 y}{\partial t^2} = w\,(x,\,t). \qquad (2)$$

The solution of eq. (2) by separation of variables has the form (Ref. 1,2,3):

$$y(x, t) = \sum_{n=1}^{\infty} \phi_n(x)\, q_n(t) \tag{3}$$

$\phi_n(x)$ is the nth modal shape or characteristic function and $q_n(t)$ the nth generalized coordinate.

Define the generalized masses and forces as:

$$M_n = \int_0^1 \rho A [\phi_n(x)]^2 \, dx \tag{4}$$

$$Q_n(t) = \int_0^1 \phi_n(x)\, w(x, t)\, dx. \tag{5}$$

Then, by virtue of an orthogonality condition, the generalized coordinates are the solutions of the ordinary differential equations:

$$M_n \ddot{q}_n(t) + M_n \omega_n^2 q_n(t) = Q_n(t). \tag{6}$$

Define the dynamic amplification factors as:

$$u_n(t) = \omega_n \int_0^t a_n(\tau) \sin \omega_n (t - \tau)\, d\tau$$

$$a_n(t) = \frac{Q_n(t)}{Q_{n\,max}} \tag{7}$$

The solution of the equation of motion, eq. (2), in terms of the defined quantities, is:

$$y\,(x,\,t) = \sum_{n=1}^{\infty} \phi_n(x)\,\frac{Q_{n\,max}}{M_n\,\omega_n^2}\,u_n(t). \tag{8}$$

The quantities of eq. (8) have a simple physical significance. $\frac{Q_{n\,max}}{M_n\omega_n^2}\,u_n(t)$ is the response of a single degree of freedom oscillator such as is shown in Fig. 1. Since $M_n\,\omega_n^2$ is the spring constant of the oscillator, $\frac{Q_{n\,max}}{M_n\,\omega_n^2}$ is the static response to the maximum force. $u_n(t)$ is the usual dynamic amplification factor which is the ratio of the dynamic response to the maximum static response.

From a structural viewpoint, the elastic forces are usually of more interest than the displacements. From elementary beam theory, the bending moment and shear force are:

$$M\,(x,\,t) = EI \sum_{n=1}^{\infty} \frac{d^2\phi_n(x)}{dx^2}\;\frac{Q_{n\,max}}{M_n\,\omega_n^2}\;u_n(t) \tag{9}$$

$$V\,(x,\,t) = EI \sum_{n=1}^{\infty} \frac{d^3\phi_n(x)}{dx^3}\;\frac{Q_{n\,max}}{M_n\,\omega_n^2}\;u_n(t) \tag{10}$$

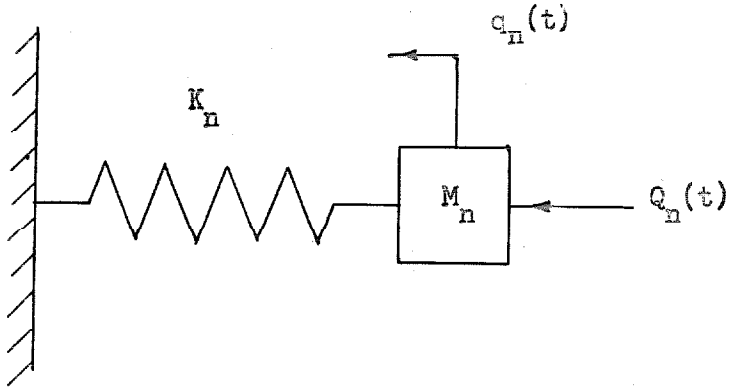

M_n Generalized Mass

$K_n = M_n \omega_n^2$, Generalized Spring Constant

$Q_n(t)$ Generalized Force

$q_n(t)$ Generalized Coordinate

FIGURE 1

THE SINGLE DEGREE OF FREEDOM NATURE OF A MODE OF VIBRATION.

The bending and shear stresses can be easily obtained from the bending moment or shear force by the assumption of a stress distribution.

An alternative formulation of the solution has the advantage of more rapid mode convergence (Ref. 3,4). This formulation separates the solution into two parts, one of which is the static solution to the applied force at each instant. The other part of the solution may be called the dynamic part since it is a function of the rapidity of loading relative to the natural periods of the beam. The alternative formulation of the solution is:

$$y(x, t) = y_{dyn}(x, t) + y_{stat}(x, t)$$

$$y_{dyn}(x, t) = \sum_{n=1}^{\infty} \phi_n(x) \frac{Q_{n\,max}}{M_n \omega_n^2} [u_n(t) - a_n(t)] \tag{11}$$

$$M(x, t) = M_{dyn}(x, t) + M_{stat}(x, t)$$

$$M_{dyn}(x, t) = EI \sum_{n=1}^{\infty} \frac{d^2\phi_n(x)}{dx^2} \frac{Q_{n\,max}}{M_n \omega_n^2} [u_n(t) - a_n(t)] \tag{12}$$

$$V(x, t) = V_{dyn}(x, t) + V_{stat}(x, t)$$

$$V_{dyn}(x, t) = EI \sum_{n=1}^{\infty} \frac{d^3\phi_n(x)}{dx^3} \frac{Q_{n\,max}}{M_n \omega_n^2} [u_n(t) - a_n(t)] \tag{13}$$

The quantity $a_n(t)$ is defined by eq. (7). The subscripts stat and dyn refer to the static and dynamic parts of the solution. The static solution to the applied force can be obtained by elementary beam theory.

2. Discussion of Basic Tabulations.

An important advantage of the form of the solution is that the quantities in the solution can be tabulated for a number of situations in a concise form.

For example, the mode shapes $\phi_n(x)$ and their derivatives are functions of the beam boundary conditions only. There are six common types of beams classified with respect to boundary conditions — clamped-clamped, clamped-free, clamped-pinned, free-free, free-pinned, and pinned-pinned. Tabulation of the mode shapes and their derivatives for these six types will supply that part of the solution for most dynamic beam problems.

Similarly the other quantities in eqs. (8) through (13) are dependent on only a part of the total conditions placed on the beam. A number of basic tabulations can be assembled which will yield the solution in the majority of dynamic beam problems.

The mode shapes $\phi_n(x)$ and the first three derivatives are tabulated in Ref. (5) for the first five modes for five of the six common types of beams. The mode shapes for the sixth type, the pinned-pinned beam, are ordinary trigonometric sines.

The mode shapes tabulated in Ref. (5) satisfy the normalizing condition:

$$\int_0^1 \phi_n^2(x)\, dx = 1. \tag{14}$$

The general form for the nth mode shape is:

$$\phi_n(x) = C_n^{(1)} \sin \beta_n x + C_n^{(2)} \cos \beta_n x + C_n^{(3)} \sinh \beta_n x + C_n^{(4)} \cosh \beta_n x. \tag{15}$$

The dimensionless quantities $\beta_n l$, called characteristic numbers in Ref. (5), are the number of spatial radians in the harmonic portion of the nth mode shapes. The natural frequencies ω_n are functions of $\beta_n l$.

$$\omega_n = \left(\frac{c_1}{l}\right) \left(\frac{r}{l}\right) (\beta_n l)^2. \tag{16}$$

The values of $\beta_n l$ for five of the six common types of beams are tabulated in Ref. (5) for the first five modes. $\beta_n l$ for the sixth type, the pinned-pinned beam, is simply $n\pi$.

In view of the normalizing condition, eq. (14), the generalized masses defined by eq. (4) are identical with the beam mass.

The generalized forces $Q_n(t)$ are functions of the mode shapes and the spatial distribution of the applied force.

They can be obtained by an analytical or graphical integration of the defining eq. (5). For the special case of a transverse concentrated force F(t) applied at the point $x = x_1$, the generalized forces are:

$$Q_n(t) = \phi_n(x_1)\, F(t). \tag{17}$$

For the case of an applied bending moment $M_A(t)$ at the point $x = x_1$, the generalized forces are:

$$Q_n(t) = \left.\frac{d\phi_n(x)}{dx}\right|_{x=x_1} \cdot M_A(t). \tag{18}$$

The evaluation of the generalized forces $Q_n(t)$ in these special cases can be determined directly from the tabulated mode shapes and first derivatives found in Ref. (5).

The dynamic amplification factors $u_n(t)$ are functions of the time characteristics of the generalized forces relative to the natural frequencies ω_n. They can be determined by an analytical or graphical integration of eq. (7). The solution for the special case of a half sine wave pulse will be considered in this paper. A graph of this special pulse is shown in Fig. 2. A single pulse force such as this was chosen because the simplicity of the solution affords a clear insight into the nature of the transient response. A step pulse was

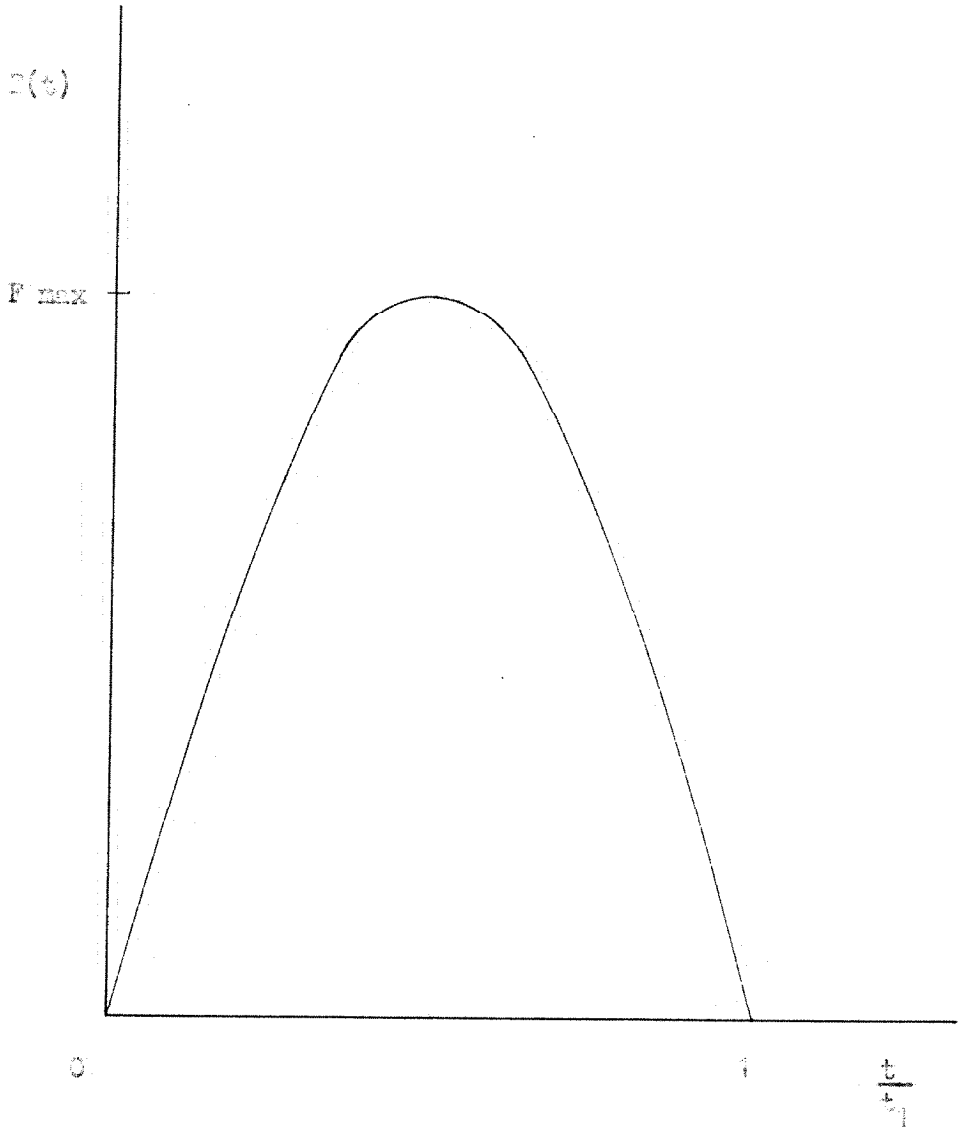

FIGURE 2

HALF SINE WAVE TRANSIENT FORCE.

not chosen because a variation of pulse duration does not change the rate of loading and unloading. Variation of the half sine wave pulse duration changes the rate of loading and unloading and results in variation of response from impulsive to static. The integration of eq. (7) for the special case of a half sine wave pulse yields:

$$u_n(t) = \frac{1}{\frac{\pi}{\omega_n t_1} - \frac{\omega_n t_1}{\pi}} \left[\sin \omega_n t - \frac{\omega_n t_1}{\pi} \sin \pi \frac{t}{t_1}\right] \quad \text{for } 0 \leq \frac{t}{t_1} \leq 1 \qquad (19)$$

$$u_n(t) = \frac{1}{\frac{\pi}{\omega_n t_1} - \frac{\omega_n t_1}{\pi}} \left[(1 + \cos \omega_n t_1) \sin \omega_n t - \sin \omega_n t_1 \cos \omega_n t\right] \quad \text{for } \frac{t}{t_1} \geq 1. \qquad (20)$$

The coefficients

$$\frac{1}{\frac{\pi}{\omega t_1} - \frac{\omega t_1}{\pi}}, \quad \frac{\frac{\omega t_1}{\pi}}{\frac{\pi}{\omega t_1} - \frac{\omega t_1}{\pi}}, \quad \frac{1 + \cos \omega t_1}{\frac{\pi}{\omega t_1} - \frac{\omega t_1}{\pi}},$$

and

$$\frac{\sin \omega t_1}{\frac{\pi}{\omega t_1} - \frac{\omega t_1}{\pi}}$$

are tabulated as functions of ωt_1 on Figs. 3 and 4. It will be noted that the first two coefficients become discontinuous at $\omega t_1 = \pi$. It was therefore necessary to plot the amplification factors u(t) in the neighborhood of $\omega t_1 = \pi$ for $0 \leq \frac{t}{t_1} \leq 1$ on Fig. 5.

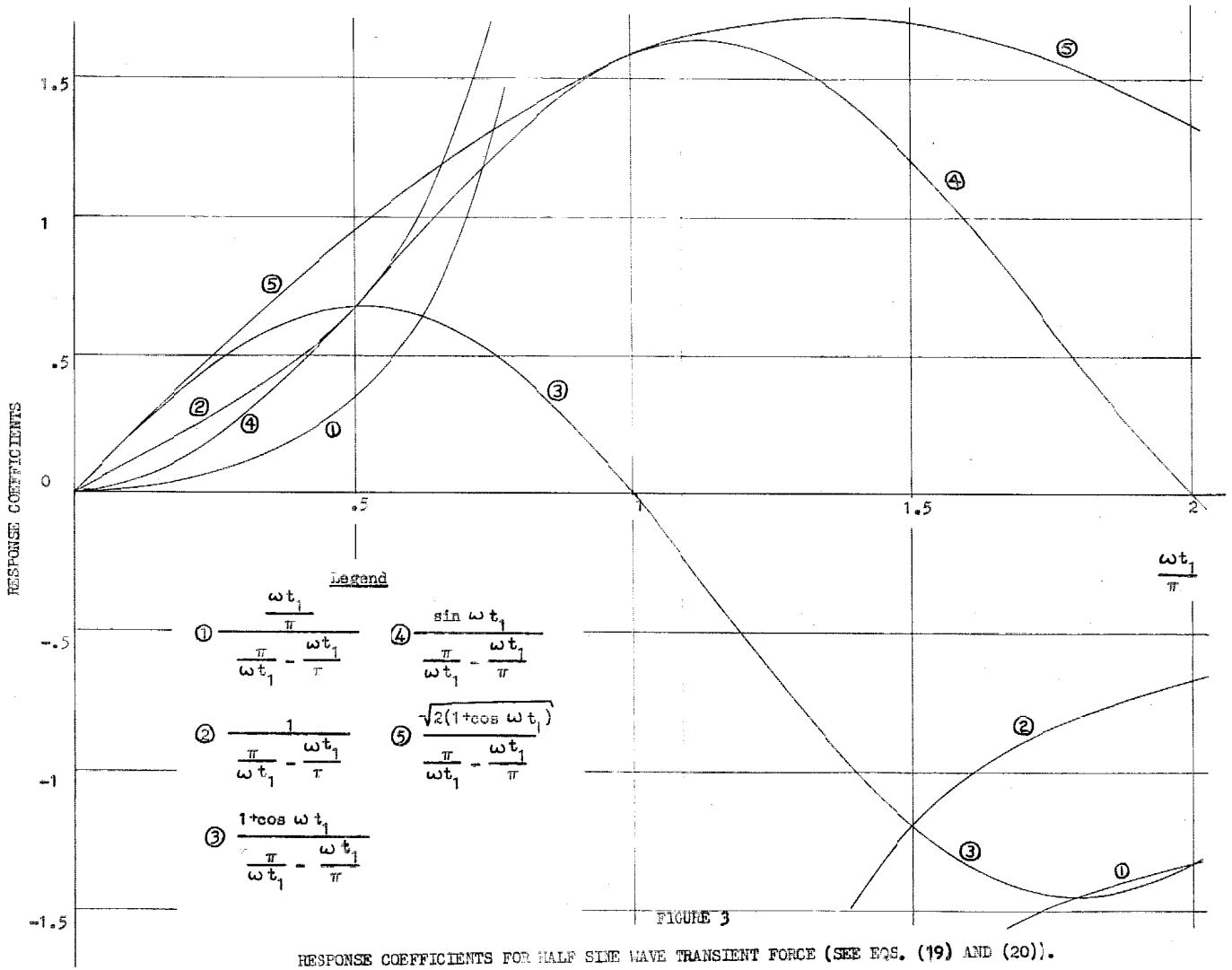

FIGURE 3

RESPONSE COEFFICIENTS FOR HALF SINE WAVE TRANSIENT FORCE (SEE EQS. (19) AND (20)).

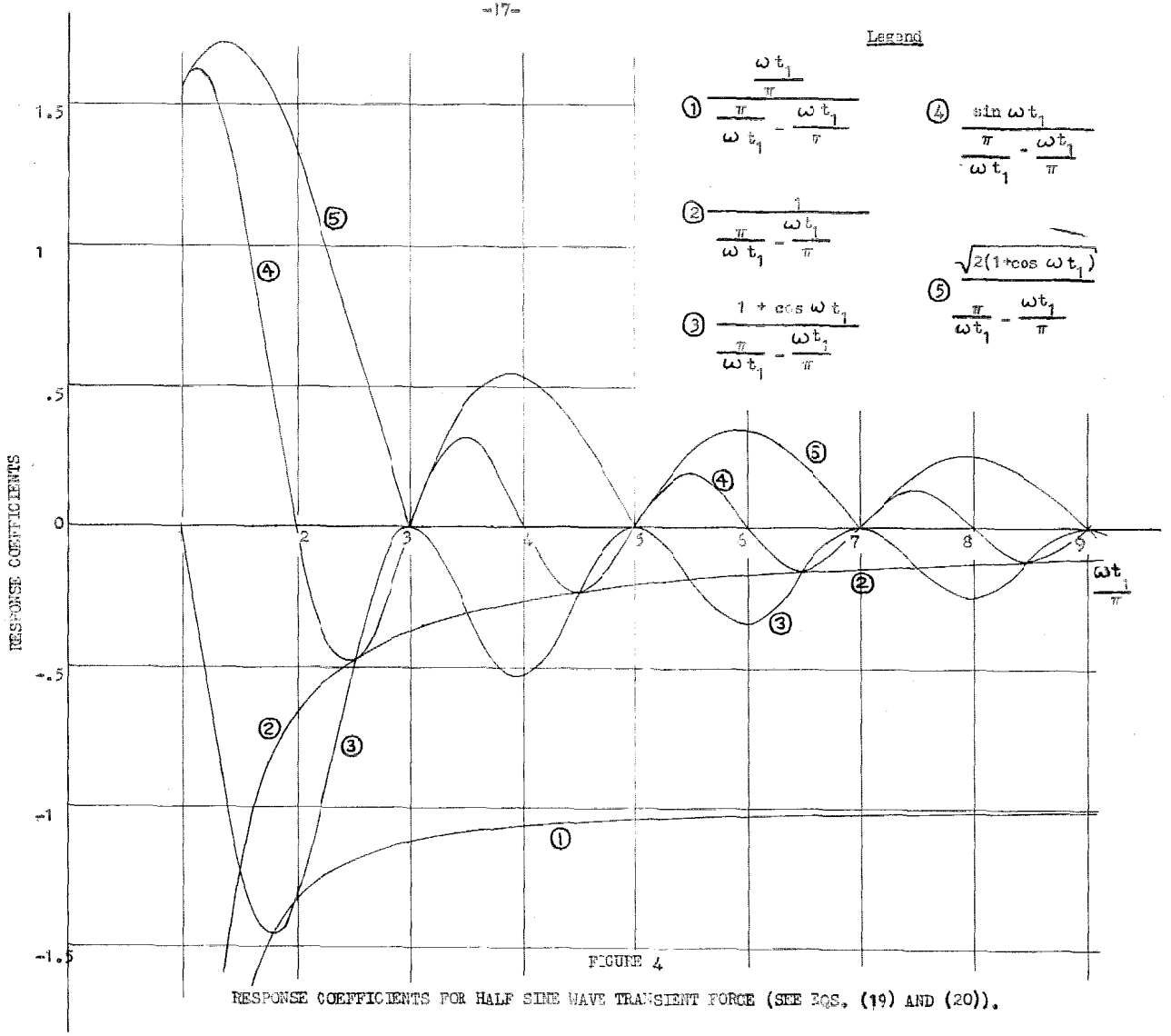

FIGURE 4

RESPONSE COEFFICIENTS FOR HALF SINE WAVE TRANSIENT FORCE (SEE EQS. (19) AND (20)).

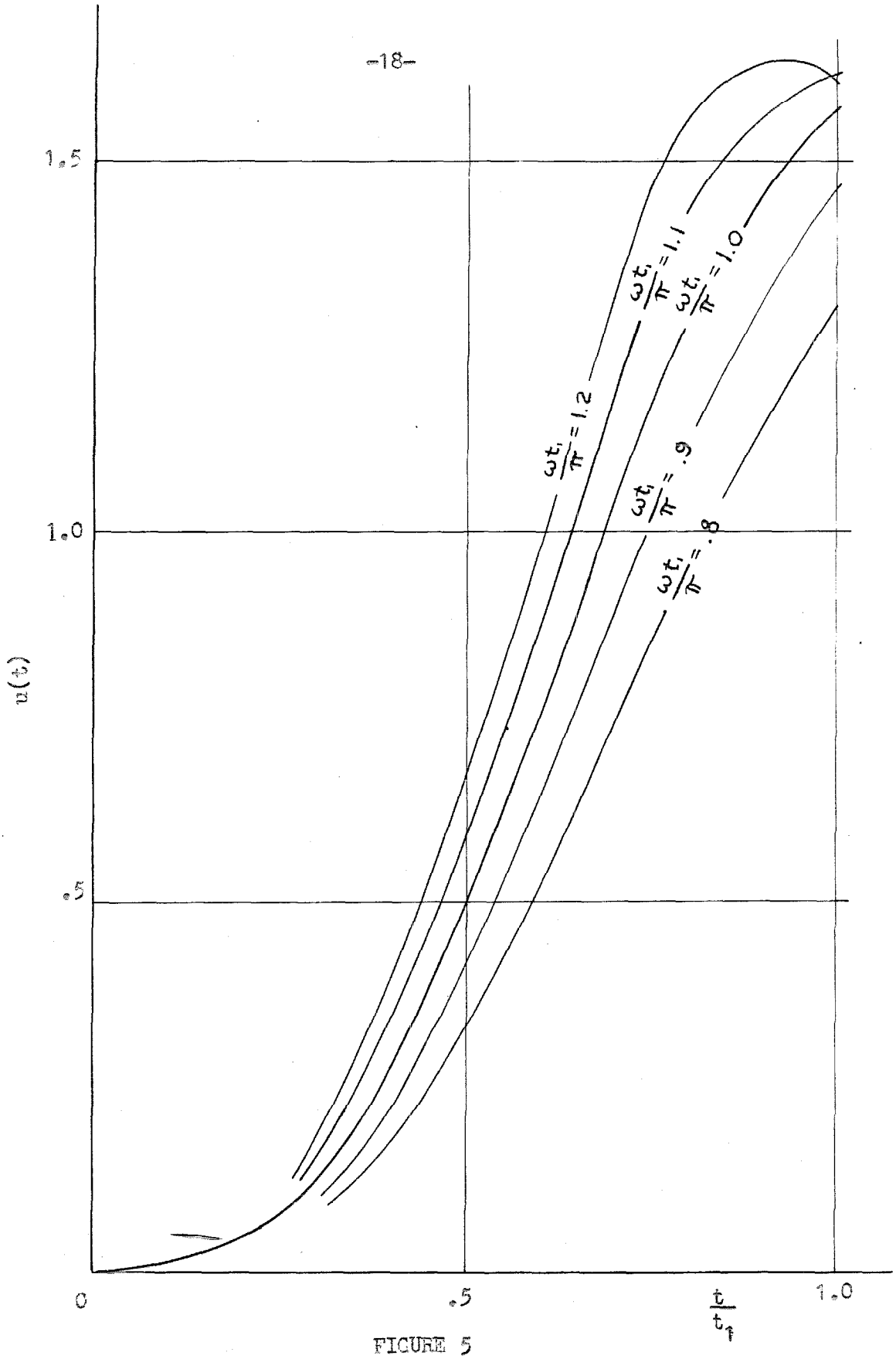

FIGURE 5

u(t) NEAR THE DISCONTINUITY AT $\omega t_1 = \pi$.

3. Discussion of Relative Response in the Higher Modes. Effect of Concentration of the Transient Force in Space and in Time.

The modal technique of dynamic beam analysis is a useful, efficient method if the convergence of mode response is sufficiently rapid that only a reasonable number of modes need be considered. It is important, then, to consider the convergence of mode response for various circumstances in order that the region of usefulness of the method may be defined.

The effect of the variation in spatial distribution and time characteristics of the transient force on the convergence of mode response will be considered. Specifically, the effect of the concentration of the transient force in space and in time will be determined.

In studying the effect of concentration of the transient force in time, Fig. 6 will be useful. This is a plot of the maximum dynamic amplification factors for a half sine wave pulse as a function of the significant parameter ωt_1. The maxima are shown for two periods of time — during the loading and subsequent to the loading. Large ωt_1 corresponds to essentially static response. For $\omega t_1 < \pi$, the response

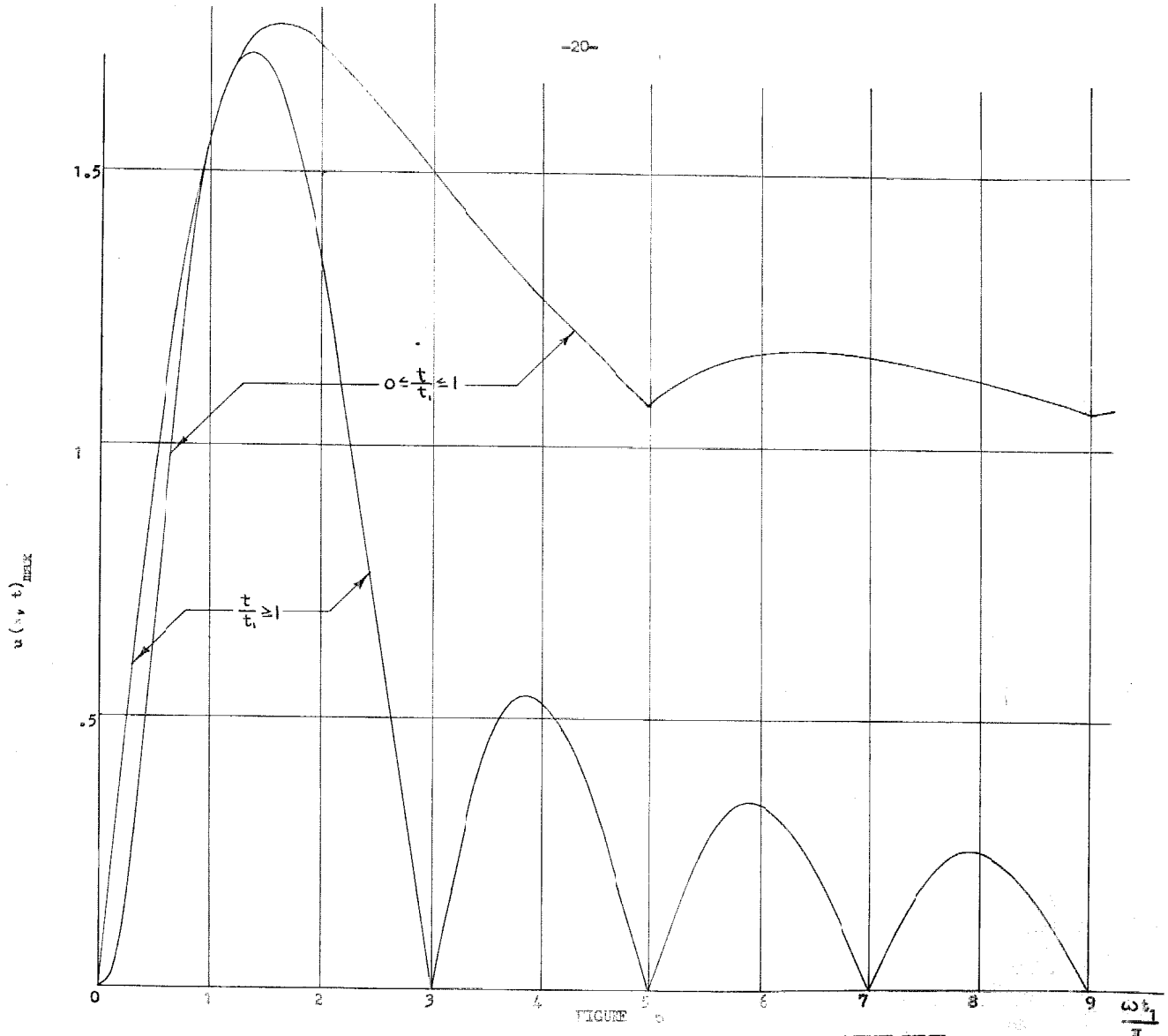

FIGURE 5

MAXIMUM DYNAMIC AMPLIFICATION FACTORS FOR HALF SINE WAVE TRANSIENT FORCE.

is essentially impulsive.

Case of a Spatially Concentrated, Transverse, Half Sine Wave Pulse.

Consider the effect of a variation in the time duration of the force on the relative response in the higher modes. If the force is slowly applied and the response is essentially static in all the modes, it can be shown from eqs. (9) and (10) that the contribution of the nth mode to the shear force and bending moment responses is of the order:

$$\text{For } 0 \leq \frac{t}{t_1} \leq 1 \qquad (M(x, t))_n \sim \frac{1}{n^2}$$

$$(V(x, t))_n \sim \frac{1}{n}$$

$$\text{For } \frac{t}{t_1} \geq 1 \qquad (M(x, t))_n \sim \frac{1}{n^3}$$

$$(V(x, t))_n \sim \frac{1}{n^2} . \qquad (21)$$

The mode convergence indicated by eqs. (21) is an envelope. None of the modes will contribute more than this. The solution convergence is actually better than indicated by eqs. (21) because, at any point on the beam, some of the modes will be positive and some negative. In order to establish the validity of eqs. (21), it is only necessary to study the quantities in

eqs. (9) and (10). If the mode shapes $\phi_n(x)$ are normalized by eq. (14), the second and third derivatives vary as n^2 and n^3. The maximum generalized forces $Q_n$max are of the order of F max. The generalized masses are identically equal. The natural frequencies ω_n vary as n^2. If the response is essentially static, the maximum dynamic amplification factors approach unity for the period $0 \leq \frac{t}{t_1} \leq 1$ and diminish within an envelope $\frac{1}{n}$ for the period $\frac{t}{t_1} \geq 1$. The mode convergence given by eqs. (21) occurs when all the natural frequencies yield values of the parameter ωt_1 well to the right of the hump in Fig. 6.

If the force is rapidly applied, some of the modes may be essentially impulsively excited. These modes are those for which $\omega t_1 < \pi$. For $\omega t_1 \ll 1$, the contribution of the nth mode to the shear force and bending moment responses is of the order:

$$\begin{aligned} &\text{For } 0 \leq \frac{t}{t_1} \leq 1 \qquad (M(x, t))_n \sim n^2 \\ &\qquad\qquad\qquad\qquad\quad (V(x, t))_n \sim n^3 \\ &\text{For } \frac{t}{t_1} \geq 1 \qquad\quad (M(x, t))_n \sim 1 \\ &\qquad\qquad\qquad\qquad\quad (V(x, t))_n \sim n \ . \end{aligned} \tag{22}$$

For $\omega t_1 < \pi$ but not small, the mode divergence is more nearly:

$$\text{For } \frac{t}{t_1} \geq 0 \qquad (M(x, t))_n \sim 1$$

$$(V(x, t))_n \sim n. \tag{23}$$

It is evident from eqs. (22) and (23) that, when some of the modes are essentially impulsively excited, the response in these modes must all be calculated. Even in the most rapid loading problem, however, only a finite number of modes will be impulsively excited. All the higher modes will approach static excitation. The convergence of the mode response in these higher modes is given by eqs. (21). The convergence is good enough that only a few of the essentially statically excited higher modes need be considered.

A more graphic presentation of the effect of the concentration in time of a spatially concentrated force is given in Fig. 7. The comparative response in a number of the modes was calculated for the special case of a pin-ended beam with a concentrated half sine wave pulse applied at the midspan for the static case, the case where $\omega_1 t_1 = \pi/10$, and the impulsive case. The static and impulsive cases behave as predicted by eqs. (21) and (22). The case where $\omega_1 t_1 = \pi/10$ roughly follows eqs. (22) and (23) for the first few modes and eqs. (21) for the higher modes.

	Bending Moment				Shear Force			
		$\omega t_1 = \pi/10$				$\omega t_1 = \pi/10$		
n	Static	$0 \leq \frac{t}{t_1} \leq 1$	$\frac{t}{t_1} \geq 1$	Impulsive	Static	$0 \leq \frac{t}{t_1} \leq 1$	$\frac{t}{t_1} \geq 1$	Impulsive
1	100	16.56	100	100	100	16.56	100	100
3	11.11	82.42	80.58	100	33.33	247.3	241.7	300
5	4.000	30.08	8.78	100	20	150.4	43.9	500
7	2.041	10.73	1.13	100	14.29	75.06	7.90	700
9	1.235	6.395	.852	100	11.11	57.56	7.67	900
11	.8264	4.153	.179	100	9.091	45.70	1.96	1100
21	.2268	1.097	.021	100	4.762	23.04	.44	2100
31	.1041	.4974	.0090	100	3.226	15.42	.28	3100
51	.0385	.1827	.0008	100	1.961	9.316	.041	5100

(Expressed as percent of first mode response).

FIGURE 7

MAXIMUM MODEWISE RESPONSES, PIN-ENDED BEAM,

CONCENTRATED HALF SINE WAVE TRANSIENT FORCE AT THE MIDPOINT.

Case of a Spatially Concentrated, Half Sine Wave, Bending Moment Pulse.

The contribution of the nth mode to the shear force and bending moment responses is given in this case by eqs. (21) through (23) if they are all multiplied by n. The only quantities in eqs. (9) and (10) which are different from the case of a concentrated force are the generalized forces. In this case, the generalized forces are given by eq. (18) and are proportional to the first derivatives of the mode shapes. Since the first derivatives vary as n, the maximum generalized forces are of the order nF max.

It is evident that an applied bending moment excites the higher modes more than do spatially concentrated forces. A more graphic presentation of the response to an applied bending moment relative to the response to a spatially concentrated force is given in Fig. 8. A modewise comparison of only the static response is shown since cases of response to more rapid loading show the same relationship.

Case of a Uniformly Distributed, Transverse, Half Sine Wave Pulse.

The contribution of the nth mode to the shear force and bending moment responses is given in this case by eqs. (21) through (23) if they are all multiplied by $\frac{1}{n}$ provided that the

	Concentrated Force		Bending Moment	
n	Bending Moment	Shear Force	Bending Moment	Shear Force
1	100	100	100	100
3	11.11	33.33	33.33	100
5	4.000	20	20	100
7	2.041	14.29	14.29	100
9	1.235	11.11	11.11	100
11	.8264	9.091	9.091	100
21	.2268	4.762	4.762	100
31	.1041	3.226	3.226	100
51	.03845	1.961	1.961	100

(Expressed as percent of first mode response).

FIGURE 8

MAXIMUM MODEWISE RESPONSES, PIN-ENDED BEAM, CONCENTRATED HALF SINE WAVE SLOWLY APPLIED FORCE AT THE MIDPOINT OR BENDING MOMENT AT THE END.

nth mode standing wave length is short relative to the length of distribution of the force. For those modes in which the standing wave length is long relative to the length of distribution of the force, eqs. (21) through (23) are more nearly correct.

The only quantities in eqs. (9) and (10) which are different from the case of a concentrated force are the generalized forces. A little thought on eq. (5) will reveal that the generalized forces are of the order $\frac{1}{n}$ F max for those higher modes where the mode standing wave lengths are short relative to the length of force distribution.

It is evident that distributed forces excite the higher modes less than do spatially concentrated forces. Fig. 9 presents a comparison of the response to a distributed force with the response to a concentrated force. The special case is that of a pin-ended beam with a transverse, spatially concentrated force applied at the midpoint or distributed uniformly around this point. A modewise comparison of only the static response is shown since cases of response to more rapid loading show the same relationship.

	Concentrated Force		Distributed Force			
			$\Delta = 1/20$		$\Delta = 1/4$	
n	Bending Moment	Shear Force	Bending Moment	Shear Force	Bending Moment	Shear Force
1	100	100	100	100	100	100
3	11.11	33.33	11.02	33.06	8.942	26.83
5	4.000	20	3.902	19.51	1.931	9.657
7	2.041	14.29	1.941	13.59	.2915	2.041
9	1.235	11.11	1.136	10.23	.1372	1.235
11	.8264	9.091	.7281	8.010	.1814	1.995
21	.2268	4.762	.1372	2.881	.0261	.5474
31	.1041	3.226	.0278	.8620	.0034	.1041
51	.0385	1.961	.0062	.3182	.0018	.0828

(Expressed as percent of first mode response).

Δ = length of distribution of force.

FIGURE 9

MAXIMUM MODEWISE RESPONSES, PIN-ENDED BEAM, CONCENTRATED OR DISTRIBUTED SLOWLY APPLIED HALF SINE WAVE TRANSIENT FORCE AT THE MIDPOINT.

SUMMARY

The effect of the concentration of a transient force in time is shown by eqs. (21) through (23). Where the force duration is long relative to the natural periods, eqs. (21) state the mode convergence. If the force duration is short relative to the natural periods, the statements of mode divergence, eqs. (22) and (23), apply to the lower modes. The shorter the force duration, the more mode responses that will obey eqs. (22) and (23).

The effect of replacing the spatially concentrated force by a concentrated bending moment is to apply a divergence factor n to eqs. (21) through (23).

The effect of distributing uniformly a force in space is to apply an attenuation factor $\frac{1}{n}$ to the higher modes whose standing wave lengths are short relative to the length of force distribution.

The divergence factors caused by the concentration of the force in space or time or by the substitution of a bending moment for the force result in a larger number of significant modes. In physically possible cases, however, the number of significant modes is always finite. This is true because it is not possible to concentrate a force or a moment to a point in space or time. There will always exist higher modes upon which the force will act as a distributed force.

4. Discussion of the Total Response.

In the preceding section the relative response in the individual modes was discussed. This leads logically to the consideration of the total response. The study of the total response will involve the summation of the significant individual mode responses.

It is particularly important to consider the total response since it appears that a popular conception concerning it is not true. This is the idea that the dynamic response of an elastic structure to a rapidly or suddenly applied force is always less than twice the response to an equivalent force statically applied (Ref. 6). It is apparent from Frankland's work that this is not true (Ref. 7).

The quantity that will be discussed here will be called the "dynamic load factor". It is defined as the ratio of the maximum dynamic response at a point alternatively to either (1) the maximum static response at the point or (2) the overall maximum static response. It is believed that the overall maximum dynamic load factor defined by (2) will be the more valuable as a design criterion since it is the best measure of the most severe condition in the structure. In this section, the dynamic load factor will be referred to

as DLF(x) with appropriate subscripts -- M or V to indicate bending moment or shear force, D to indicate small damping, and 1 or 2 to indicate which definition applies.

A general discussion of dynamic load factors in as simple an elastic structure as a uniform beam is difficult. Here, only a few especially severe cases can be discussed. A step force was chosen since it produces relatively simple results, is severe, and since it is an addition to Frankland's discussion where step excitation was also used.

The Case of a Spatially Concentrated, Step Force Applied at the Midspan of a Pin-Ended Beam.

The dynamic load factors for the bending moment are, from eq. (12):

$$[DLF(x)]_{M1} = 1 + \frac{4l}{x}\left[\sum_{n=1}^{\infty}(-1)^n \frac{\sin\frac{(2n-1)\pi x}{l}\cos\omega_{(2n-1)}t}{(2n-1)^2\pi^2}\right]_{\text{time max.}} \tag{24}$$

$$[DLF(x)]_{M2} = \frac{2x}{l} + 8\left[\sum_{n=1}^{\infty}(-1)^n \frac{\sin\frac{(2n-1)\pi x}{l}\cos\omega_{(2n-1)}t}{(2n-1)^2\pi^2}\right]_{\text{time max.}} \tag{25}$$

It should be noted that the maxima indicated in eqs. (24)

and (25) are time maxima. It does not appear to be feasible or possible to evaluate series of the type in eqs. (24) and (25) analytically. The series will evidently have to be summed graphically. Things to be considered in such a summation will be discussed next.

First, a series in which the absolute values of the terms form a divergent series cannot be treated since there would be no limit to the number of terms which must be summed. Second, it is necessary to determine whether the series is periodic in time or not. If the series is periodic, it is only necessary to plot the terms of the series through one period. If the series is non-periodic in time, this is not possible. In either case, an upper bound can be obtained by taking the sum of the absolute, time-maximum values of the terms in the series.

In the special case of a pin-ended beam, the natural frequencies all bear an integer relationship to the fundamental frequency. In this case, it is evident that the series of eqs. (24) and (25) are periodic in time with the period of the fundamental. The terms of eqs. (24) and (25) vary as $\frac{1}{n^2}$ and the series is always convergent. The series can be evaluated by plotting the significant terms during a fundamental period and summing.

However, this is laborious and it is easier to consider first the bounding values of eqs. (24) and (25). The bounding value of the series is the sum of the absolute, time-maximum, values of the terms. The bounding values of eqs. (24) and (25) are:

$$[DLF(x)]_{M1} \leq 1 + \frac{4l}{x} \sum_{n=1}^{\infty} \frac{\left|\sin \frac{(2n-1)\pi x}{l}\right|}{(2n-1)^2 \pi^2} \qquad \text{for } 0 \leq x \leq 1/2 \qquad (26)$$

$$[DLF(x)]_{M2} \leq \frac{2x}{l} + 8 \sum_{n=1}^{\infty} \frac{\left|\sin \frac{(2n-1)\pi x}{l}\right|}{(2n-1)^2 \pi^2} \qquad \text{for } 0 \leq x \leq 1/2 \qquad (27)$$

Eqs. (26) and (27) were evaluated for a number of points on the beam and were plotted on Fig. 10, labeled $\frac{c}{c_c} = 0$. The dynamic load factors, defined by eqs. (24) and (25), were also plotted on Fig. 10 for x = 1/8 for the undamped case $\frac{c}{c_c} = 0$.

An examination of the curves labeled $\frac{c}{c_c} = 0$ on Fig. 10 reveals that the bounding value of the dynamic load factor, $[DLF(x)]_{M1}$ is always greater than two except at the loading point where it is identically two. The bounding value of the dynamic load factor, $[DLF(x)]_{M2}$, is always less than two except at the loading point where it is identically two. At the time $t = \pi/\omega_1$, eqs. (24) and (25) are equal to 2 and 4x/l.

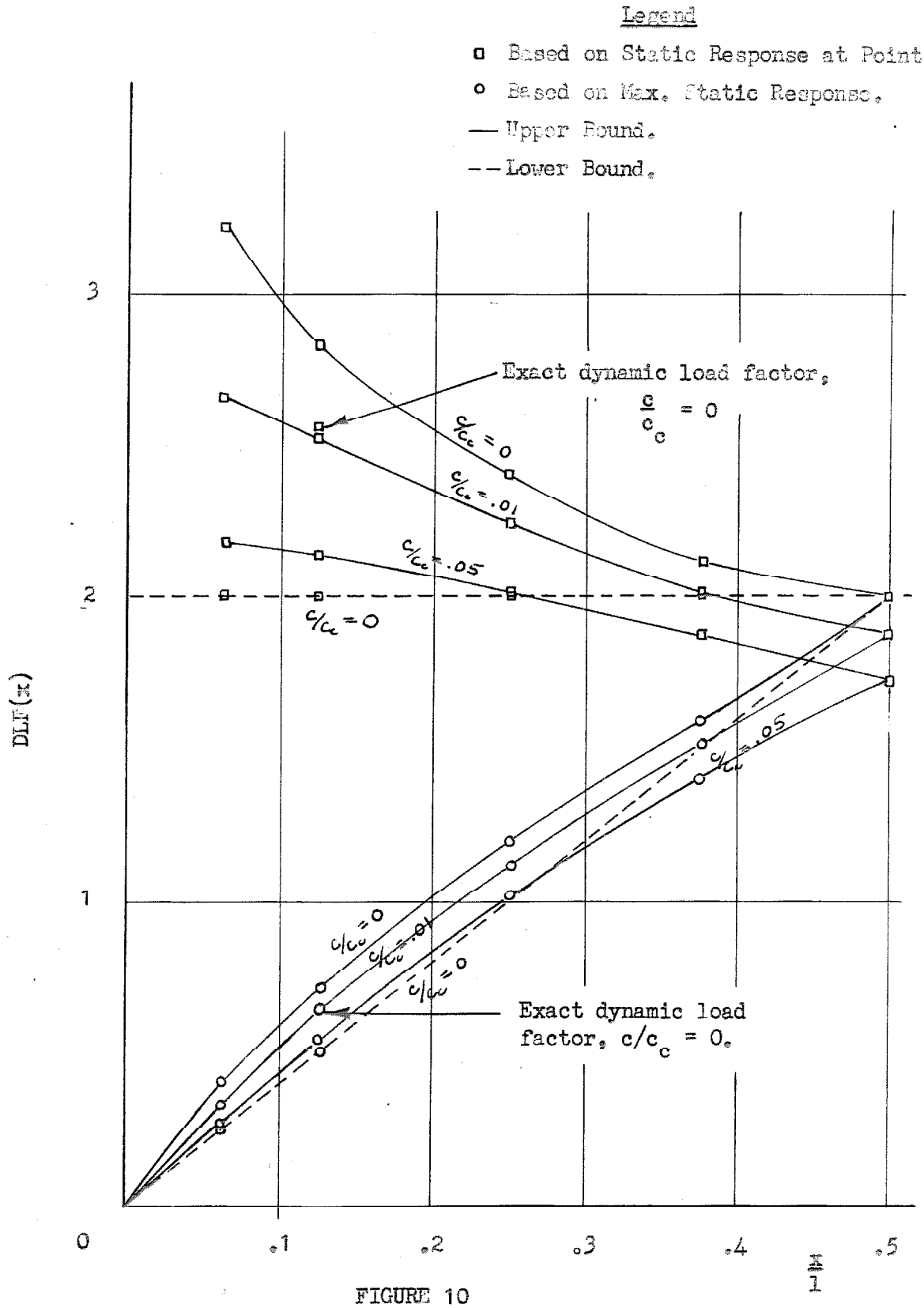

FIGURE 10

DYNAMIC LOAD FACTOR BOUNDS, BENDING MOMENT RESPONSE, PIN-ENDED BEAM, CONCENTRATED STEP FORCE.

These values are lower bounds on the dynamic load factors and are shown on Fig. 10

It was desired to obtain some measure of the effect of small damping on the dynamic load factors. One of the conclusions of Mindlin and others (Ref. 8) was that the initial mode responses were insensitive to the law of damping for small damping. Another conclusion was that the damping expressed as a percent of critical damping appeared to be the same in all the modes. With this in mind, the effect of small damping was taken into account by applying to each term of the series of eqs. (24) and (25) the decay function $e^{-\frac{c}{c_c}\omega_{(2n-1)}t}$

$$[DLF(x)]_{MD1} = 1 + \frac{4l}{x}\left[\sum_{n=1}^{\infty}(-1)^n e^{-\frac{c}{c_c}\omega_{(2n-1)}t} \cdot \frac{\sin\frac{(2n-1)\pi x}{l}\cos\omega_{(2n-1)}t}{(2n-1)^2\pi^2}\right]_{\substack{\text{time}\\ \text{max.}}}$$

$$\text{for } 0 \le x \le 1/2 \qquad (28)$$

$$[DLF(x)]_{MD2} = \frac{2x}{l} + 8\left[\sum_{n=1}^{\infty}(-1)^n e^{-\frac{c}{c_c}\omega_{(2n-1)}t} \cdot \frac{\sin\frac{(2n-1)\pi x}{l}\cos\omega_{(2n-1)}t}{(2n-1)^2\pi^2}\right]_{\substack{\text{time}\\ \text{max.}}}$$

$$\text{for } 0 \le x \le 1/2 \qquad (29)$$

Eqs. (28) and (29) can be evaluated graphically. However, it is easier to consider bounding values.

Since the fundamental mode predominates in the solution, the series in eqs. (28) and (29) will, for small damping, be maximum in the neighborhood of the time when the fundamental mode reaches its first maximum, $t = \pi/\omega_1$. A close approximation to the bounding values of eqs. (28) and (29) can be achieved by evaluating the series of the absolute, time-maximum, values of the terms at the time $t = \pi/\omega_1$.

$$[DLF(x)]_{MD1} \leq 1 + \frac{4l}{x} \sum_{n=1}^{\infty} e^{-\frac{c}{c_c}\frac{\omega_{(2n-1)}}{\omega_1}\pi} \cdot \frac{\left|\sin\frac{(2n-1)\pi x}{l}\right|}{(2n-1)^2\pi^2}$$

for $0 \leq x \leq l/2$ (30)

$$[DLF(x)]_{MD2} \leq \frac{2x}{l} + 8 \sum_{n=1}^{\infty} e^{-\frac{c}{c_c}\frac{\omega_{(2n-1)}}{\omega_1}\pi} \cdot \frac{\left|\sin\frac{(2n-1)\pi x}{l}\right|}{(2n-1)^2\pi^2}$$

for $0 \leq x \leq l/2$ (31)

Eqs. (30) and (31) were evaluated for a number of points on the beam and for values of $\frac{c}{c_c}$ of 0.01 and 0.05. The results were plotted on Fig. 10.

The dynamic load factors for the shear force are, by eq. (13), the identical expression:

$$[DLF(x)]_{V1,2} = 1 + 4 \left[\sum_{n=1}^{\infty} (-1)^n \frac{\cos \frac{(2n-1)\pi x}{l} \cos \omega_{(2n-1)} t}{(2n-1)\pi} \right]_{\substack{\text{time} \\ \text{max.}}} \qquad (32)$$

It is not possible to treat the dynamic load factors for the shear force in the same manner as for the bending moment since the absolute, time-maximum, values of the terms in the series vary as $1/n$, causing the series to be divergent. A bound on the dynamic load factor apparently cannot be produced. However, the lower bound is everywhere equal to two since eq. (32) is everywhere equal to two when $t = \pi/\omega_1$.

Case of Uniformly Distributed, Step Force Applied to a Pin-Ended Beam.

The dynamic load factors for the bending moment are, by eq. (12):

$$[DLF(x)]_{M1} = 1 + \frac{8l}{x(1 - \frac{x}{l})} \left[\sum_{n=1}^{\infty} \frac{-\sin \frac{(2n-1)\pi x}{l} \cos \omega_{(2n-1)} t}{(2n-1)^3 \pi^3} \right]_{\substack{\text{time} \\ \text{max.}}}$$

$$\text{for } 0 \leq x \leq 1/2 \qquad (33)$$

$$[DLF(x)]_{M2} = \frac{4x}{l}(1 - \frac{x}{l}) + 32 \left[\sum_{n=1}^{\infty} \frac{-\sin \frac{(2n-1)\pi x}{l} \cos \omega_{(2n-1)} t}{(2n-1)^3 \pi^3} \right]_{\substack{\text{time} \\ \text{max.}}}$$

$$\text{for } 0 \leq x \leq 1/2 \qquad (34)$$

The absolute values of the terms in the series in eqs. (33) and (34) form a rapidly convergent series. Since the series is periodic in the period of the fundamental mode, the dynamic load factors can be determined by a graphical summation over one fundamental period.

However, it is easier to consider the bounding values of eqs. (33) and (34). The bounding value of the series is the sum of the absolute, time-maximum values of the terms. The bounding values of eqs. (33) and (34) are:

$$[DLF(x)]_{M1} \leq 1 + \frac{8l}{x(1 - \frac{x}{l})} \sum_{n=1}^{\infty} \frac{\left|\sin \frac{(2n-1)\pi x}{l}\right|}{(2n-1)^3 \pi^3}$$

$$\text{for } 0 \leq x \leq l/2 \qquad (35)$$

$$[DLF(x)]_{M2} \leq \frac{4x}{l}\left(1 - \frac{x}{l}\right) + 32 \sum_{n=1}^{\infty} \frac{\left|\sin \frac{(2n-1)\pi x}{l}\right|}{(2n-1)^3 \pi^3}$$

$$\text{for } 0 \leq x \leq l/2 \qquad (36)$$

Eqs. (35) and (36) were evaluated at a number of points on the beam and were plotted on Fig. 11, labeled $\frac{c}{c_c} = 0$. The dynamic load factors are identical at $x = l/2$. This value was determined graphically from eqs. (33) and (34) and was plotted on Fig. 11.

Legend

□ Based on Static Response at Point.

○ Based on Max. Static Response.

—— Upper Bound.

– – Lower Bound.

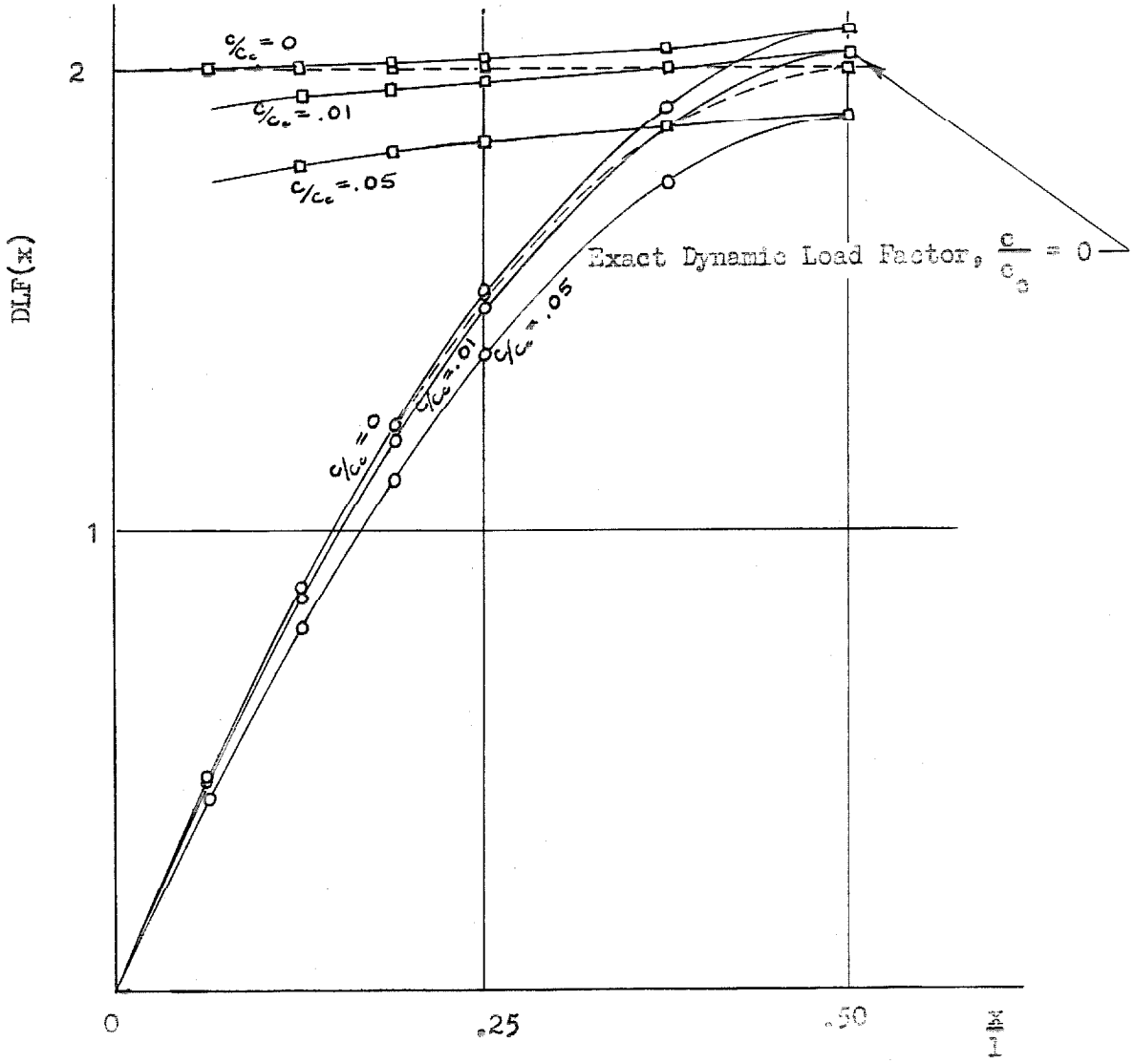

FIGURE 11

DYNAMIC LOAD FACTOR BOUNDS, BENDING MOMENT RESPONSE PIN-ENDED BEAM, UNIFORMLY APPLIED STEP FORCE.

An examination of the curves labeled $\frac{c}{c_c} = 0$ on Fig. 11 reveals that the bounding value of the dynamic load factor, $[DLF(x)]_{M1}$, is greater than two except at the ends of the beam where it is identically two. The bounding value of the dynamic load factor, $[DLF(x)]_{M2}$, is less than two except near the center of the beam where it is larger. At time $t = \pi/\omega_1$, eqs. (33) and (34) are equal to 2 and $\frac{8x}{l}(1 - \frac{x}{l})$. These values are a lower bound on the dynamic load factors and are shown on Fig. 11.

The slightly damped counterparts of eqs. (33) and (34), treated as in the case of a concentrated force, are:

$$[DLF(x)]_{MD1} = 1 + \frac{8l}{x\,(1 - \frac{x}{l})} \left[\sum_{n=1}^{\infty} -e^{-\frac{c}{c_c}\omega_{(2n-1)}t} \cdot \frac{\sin\frac{(2n-1)\pi x}{l} \cos\omega_{(2n-1)}t}{(2n-1)^3\,\pi^3} \right]_{\substack{\text{time} \\ \text{max.}}}$$

$$\text{for } 0 \le x \le l/2 \qquad (37)$$

$$[DLF(x)]_{MD2} = \frac{4x}{l}(1 - \frac{x}{l}) + 32 \left[\sum_{n=1}^{\infty} -e^{-\frac{c}{c_c}\omega_{(2n-1)}t} \cdot \frac{\sin\frac{(2n-1)\pi x}{l} \cos\omega_{(2n-1)}t}{(2n-1)^3\,\pi^3} \right]_{\substack{\text{time} \\ \text{max.}}} \quad \text{for } 0 \le x \le l/2 \qquad (38)$$

Since the fundamental mode predominates, the dynamic load factors, eqs. (37) and (38), will be maximum in the neighborhood of the time when the fundamental mode reaches its first maximum, $t=\pi/\omega_1$. A close approximation to the bounding values of eqs. (37) and (38) can be obtained by evaluating the series of the absolute, time-maximum, values of the terms at the time $t = \pi/\omega_1$.

$$[DLF(x)]_{MD1} \leq 1 + \frac{81}{x(1 - \frac{x}{l})} \sum_{n=1}^{\infty} e^{-\frac{c}{c_c}\frac{\omega_{(2n-1)}}{\omega_1}\pi} \cdot \frac{\left|\sin\frac{(2n-1)\pi x}{l}\right|}{(2n-1)^3 \pi^3} \qquad \text{for } 0 \leq x \leq l/2 \tag{39}$$

$$[DLF(x)]_{MD2} \leq \frac{4x}{l}(1 - \frac{x}{l}) + 32 \sum_{n=1}^{\infty} e^{-\frac{c}{c_c}\frac{\omega_{(2n-1)}}{\omega_1}\pi} \frac{\left|\sin\frac{(2n-1)\pi x}{l}\right|}{(2n-1)^3 \pi^3} \qquad \text{for } 0 \leq x \leq l/2 \tag{40}$$

Eqs. (39) and (40) were evaluated for a number of points on the beam and for values of $\frac{c}{c_c}$ of 0.01 and 0.05. The results were plotted on Fig. 11.

The dynamic load factors for the shear force are, by eq. (13):

$$[DLF(x)]_{V1} = 1 + \frac{8}{1 - 2\frac{x}{l}} \left[\sum_{n=1}^{\infty} \frac{-\cos \frac{(2n-1)\pi x}{l} \cos \omega_{(2n-1)} t}{(2n-1)^2 \pi^2} \right]_{\substack{\text{time} \\ \text{max.}}}$$

$$\text{for } 0 \leq x \leq l/2 \qquad (41)$$

$$[DLF(x)]_{V2} = (1 - 2\frac{x}{l}) + 8 \left[\sum_{n=1}^{\infty} \frac{-\cos \frac{(2n-1)\pi x}{l} \cos \omega_{(2n-1)} t}{(2n-1)^2 \pi^2} \right]_{\substack{\text{time} \\ \text{max.}}}$$

$$\text{for } 0 \leq x \leq l/2 \qquad (42)$$

The bounding value of the series is the sum of the absolute, time-maximum, values of the terms. The bounding values of eqs. (41) and (42) are:

$$[DLF(x)]_{V1} \leq 1 + \frac{8}{1 - 2\frac{x}{l}} \sum_{n=1}^{\infty} \frac{\left|\cos \frac{(2n-1)\pi x}{l}\right|}{(2n-1)^2 \pi^2}$$

$$\text{for } 0 \leq x \leq l/2 \qquad (43)$$

$$[DLF(x)]_{V2} \leq (1 - 2\frac{x}{l}) + 8 \sum_{n=1}^{\infty} \frac{\left|\cos \frac{(2n-1)\pi x}{l}\right|}{(2n-1)^2 \pi^2}$$

$$\text{for } 0 \leq x \leq l/2 \qquad (44)$$

Eqs. (43) and (44) were evaluated for a number of points on the beam and were plotted on Fig. 12, labeled $\frac{c}{c_c} = 0$. The values of eqs. (41) and (42) when $t = \pi/\omega_1$, the lower bounds are also shown on Fig. 12.

The slightly damped counterparts of eqs. (41) and (42), treated as in the case of a concentrated force, are:

$$[DLF(x)]_{VD1} = 1 + \frac{8}{1 - 2\frac{x}{l}}\left[\sum_{n=1}^{\infty} - e^{-\frac{c}{c_c}\omega_{(2n-1)}t} \cdot \frac{\cos\frac{(2n-1)\pi x}{l}\cos\omega_{(2n-1)}t}{(2n-1)^2\ \pi^2}\right]_{\text{time max.}}$$

$$\text{for } 0 \leq x \leq 1/2 \qquad (45)$$

$$[DLF(x)]_{VD2} = (1 - 2\frac{x}{l}) + 8\left[\sum_{n=1}^{\infty} - e^{-\frac{c}{c_c}\omega_{(2n-1)}t} \cdot \frac{\cos\frac{(2n-1)\pi x}{l}\cos\omega_{(2n-1)}t}{(2n-1)^2\ \pi^2}\right]_{\text{time max.}}$$

$$\text{for } 0 \leq x \leq 1/2 \qquad (46)$$

Since the fundamental mode predominates, the dynamic load factors, eqs. (45) and (46), will be maximum in the neighborhood of the time when the fundamental reaches its first maximum, $t = \pi/\omega_1$. A close approximation to the bounding values of eqs. (45) and (46) can be obtained by evaluating the series of

Legend

□ Based on Static Stress at Point.

○ Based on Max. Static Stress.

—— Upper Bounds.

– – Lower Bounds.

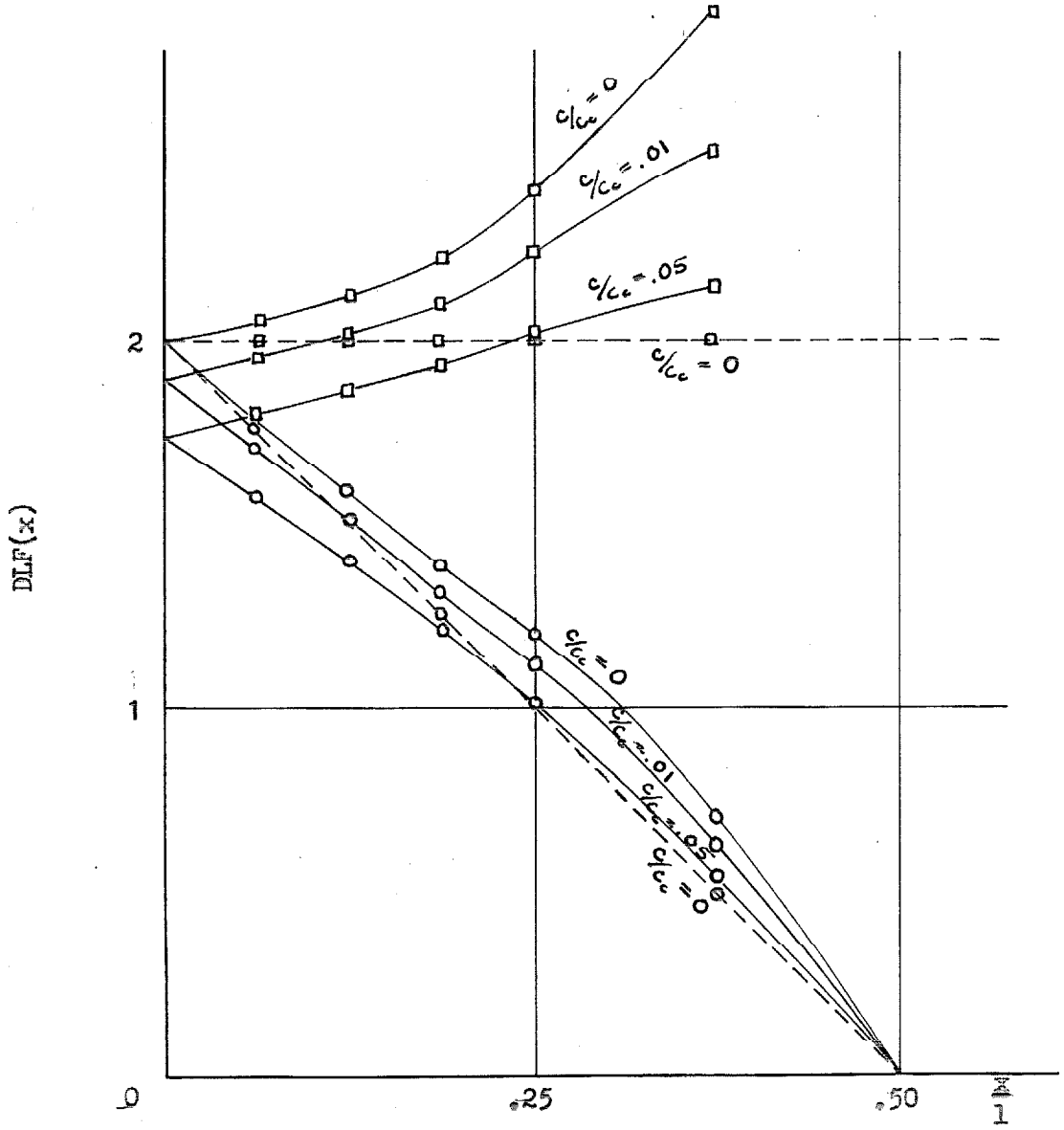

FIGURE 12

DYNAMIC LOAD FACTOR BOUNDS, SHEAR FORCE RESPONSE, PIN-ENDED BEAM, UNIFORMLY APPLIED STEP FORCE.

the absolute, time-maximum, values of the terms at the time $t = \pi/\omega_1$.

$$[DLF(x)]_{VD1} \leq 1 + \frac{8}{1 - 2\frac{x}{l}} \sum_{n=1}^{\infty} e^{-\frac{c}{c_c}\frac{\omega_{(2n-1)}}{\omega_1}\pi} \cdot \frac{\left|\cos\frac{(2n-1)\pi x}{l}\right|}{(2n-1)^2\pi^2} \qquad \text{for } 0 \leq x \leq 1/2 \tag{47}$$

$$[DLF(x)]_{VD2} \leq (1 - 2\frac{x}{l}) + 8 \sum_{n=1}^{\infty} e^{-\frac{c}{c_c}\frac{\omega_{(2n-1)}}{\omega_1}\pi} \cdot \frac{\left|\cos\frac{(2n-1)\pi x}{l}\right|}{(2n-1)^2\pi^2} \qquad \text{for } 0 \leq x \leq 1/2 \tag{48}$$

Eqs. (47) and (48) were evaluated for a number of points on the beam and for values of $\frac{c}{c_c}$ of 0.01 and 0.05. The results were plotted on Fig. 12.

SUMMARY

Spatially Concentrated Step Force Applied at the Midpoint of a Pin-Ended Beam.

(1) The dynamic load factor for the bending moment referred to the maximum static bending moment at the point is larger than two except at the midpoint where it is identically two.

(2) The dynamic load factor for the bending moment referred to the overall maximum static bending moment is less than two except at the midpoint where it is identically two.

(3) The dynamic load factor for the shear force is identical when referred to either the maximum static shear force at the point or the overall maximum static shear force.

The lower bound is everywhere two. It appears to be impossible to supply an upper bound in this case.

Uniformly Applied Step Force Applied to a Pin-Ended Beam.

(1) The dynamic load factor for the bending moment referred to the maximum static bending moment at the point is larger than two except at the ends where it is identically two.

(2) The dynamic load factor for the bending moment

referred to the overall maximum static bending moment is less than two except near the midpoint where it is larger than two.

(3) The dynamic load factor for the shear force referred to the maximum static shear force at the point is larger than two except at the ends where it is identically two.

(4) The dynamic load factor for the shear force referred to the overall maximum static shear force is always less than two except at the ends where it is identically two.

The proof in (Ref. 6) that the dynamic load factors of elastic structures cannot be greater than two for rapidly or suddenly applied forces is incomplete. While it is true that none of the modes will be excited to more than twice the static response, it is not necessarily true that the total response at each point will not be greater than twice the total static response at that point. In the static response at a point some of the modes make a positive contribution and some a negative contribution. In the dynamic response, it is possible that a time may exist for each point such that the modes combine more favorably than in the static response.

It is apparent that the behavior of the dynamic load factor depends on the relative mode response. If there is a

rapid convergence of mode response, the system approaches a single degree of freedom in behavior. The "factor of two" criterion is approached in this case. The case of the most rapid mode convergence covered in this section is that of the bending moment response in the case of a distributed force in which the mode responses vary as $1/n^3$. It can be seen on Fig. 11 that the dynamic load factors are near those predicted for a single degree of freedom system.

The mode responses vary as $1/n^2$ in the bending moment response in the case of a concentrated force and the shear force response in the case of a distributed force. Figs. 10 and 12 reveal that the dynamic load factors in these cases are not close to those predicted for a single degree of freedom system.

5. Discussion of the Independence of the Boundary Conditions of the Higher Mode Responses.

In the study of transient behavior of beams, it is generally most convenient to study the response in the particularly simple case of a pin-ended beam. If it can be shown that the higher mode responses approach independence to the boundary conditions, the mode responses determined for the pin-ended beam can be extended to other beams. Quantities such as the dynamic load factor, which appears to be a function of the convergence of the higher mode responses, could be extended from the case of a pin-ended beam to other beams. The concept of higher mode independence of end conditions has been used by Williams in determining higher mode shapes and frequencies (Ref. 8a).

The boundary conditions affect the transient behavior of a beam through their effect on the mode shapes. Directly or indirectly, the quantities in the solution are functions of the mode shapes. Consider then the effect of the boundary conditions on the mode shapes.

It can be shown that the higher mode shapes for the common boundary conditions -- pinned-end, free-end, built-in-end — are harmonic except for a short exponential transition near the boundaries. Consider a special case — that of a cantilever beam. Take the origin of coordinates at the built-in-end with the x axis along the equilibrium axis of the beam.

For this special case, the Bernoulli-Euler theory yields the mode shapes:

$$\phi_n(x) = A_n[\sin \beta_n x - \sinh \beta_n x - \frac{\sin \beta_n l + \sinh \beta_n l}{\cos \beta_n l + \cosh \beta_n l} (\cos \beta_n x - \cosh \beta_n x)]. \quad (49)$$

A_n is an arbitrary constant. For $\beta_n l$ large, it can be shown that, very closely:

$$\phi_n(x) \approx A_n[\sin \beta_n x - \cos \beta_n x + \sin \beta_n l \, e^{-\beta_n l(1 - \frac{x}{l})} - \cos \beta_n l \, e^{-\beta_n l(1 - \frac{x}{l})} + e^{-\beta_n x}]. \quad (50)$$

For a cantilever beam, $\beta_n l$ rapidly converges on $(n - \frac{1}{2})\pi$ as n becomes larger. In the second mode $\beta_n l$ is within 1°/o of the approximate $3/2\pi$. In view of this, eq. (50) becomes:

$$\phi_n(x) \approx A_n[\sin \frac{(n - 1/2)\pi x}{l} - \cos \frac{(n - 1/2)\pi x}{l} - (-1)^n e^{-(n - \frac{1}{2})\pi(1 - \frac{x}{l})} + e^{-(n - \frac{1}{2})\pi \frac{x}{l}}]. \quad (51)$$

The first two terms of eq. (51) are the harmonic portion of the mode shape. The other two terms are the exponential

end transitions and are negligible except near the ends.

It is convenient to find another form of eq. (51) incorporating the mode standing wave lengths. The mode standing wave lengths are:

$$\lambda_n = \frac{2l}{n - 1/2} \quad . \tag{52}$$

An alternative form of eq. (51) for the higher mode shapes is:

$$\phi_n(x) \approx A_n\left[\sin 2\pi \frac{x}{\lambda_n} - \cos 2\pi \frac{x}{\lambda_n} - (-1)^n e^{-\left[(n - \frac{1}{2})\pi - 2\pi \frac{x}{\lambda_n}\right]} + e^{-2\pi \frac{x}{\lambda_n}}\right] . \tag{53}$$

A_n was arbitrarily chosen to be unity which, in the higher modes, approaches the normalizing condition, eq. (14). Values of $\phi_n(x)$ given by eq. (53) are plotted near the ends of the beam on Fig. 13 for the odd modes. For the even modes, it is only necessary to invert the curves at one of the ends. The exponential transitions give a significant contribution for $\frac{1}{2}$ wave length, λ_n, at the ends. The exact mode shapes approach the values given by eq. (53) very rapidly as n becomes larger. The exact third mode shape for a cantilever beam is everywhere within 1 % of the approximate shape give by eq. (53).

The derivatives of the mode shapes, in the case of a cantilever beam, have expressions similar to eq. (53).

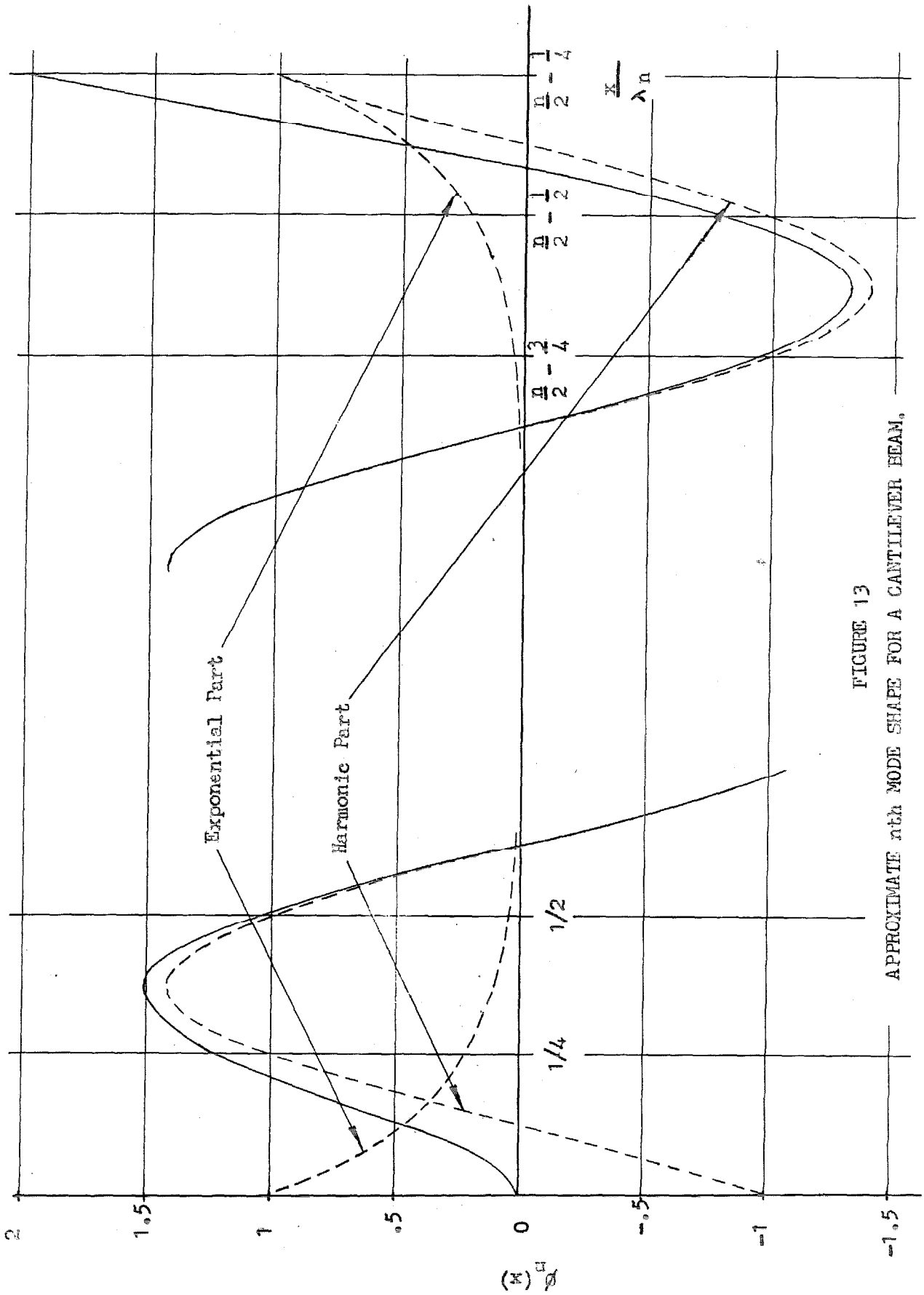

FIGURE 13

APPROXIMATE nth MODE SHAPE FOR A CANTILEVER BEAM.

In the higher modes, the first three derivatives of $\phi_n(x)$ are, approximately:

$$\frac{\frac{d\phi_n(x)}{dx}}{\beta_n} \approx A_n\left[\cos 2\pi \frac{x}{\lambda_n} + \sin 2\pi \frac{x}{\lambda_n} - (-1)^n e^{-[(n - 1/2)\pi - 2\pi \frac{x}{\lambda_n}]} - e^{-2\pi \frac{x}{\lambda_n}}\right] \quad (54)$$

$$\frac{\frac{d^2\phi_n(x)}{dx^2}}{\beta_n^2} \approx A_n\left[\cos 2\pi \frac{x}{\lambda_n} - \sin 2\pi \frac{x}{\lambda_n} - (-1)^n e^{-[(n - 1/2)\pi - 2\pi \frac{x}{\lambda_n}]} + e^{-2\pi \frac{x}{\lambda_n}}\right] \quad (55)$$

$$\frac{\frac{d^3\phi_n(x)}{dx^3}}{\beta_n^3} \approx A_n\left[-\cos 2\pi \frac{x}{\lambda_n} - \sin 2\pi \frac{x}{\lambda_n} - (-1)^n e^{-[(n - 1/2)\pi - 2\pi \frac{x}{\lambda_n}]} - e^{-2\pi \frac{x}{\lambda_n}}\right] \quad (56)$$

Values of the derivatives given by eqs. (54) through (56), for A_n unity, are plotted near the ends of the cantilever beam on Figs. 14 through 16 for the odd modes. For the even modes, it is only necessary to invert the curves at one of the ends. The exact derivatives of the third mode shape of a

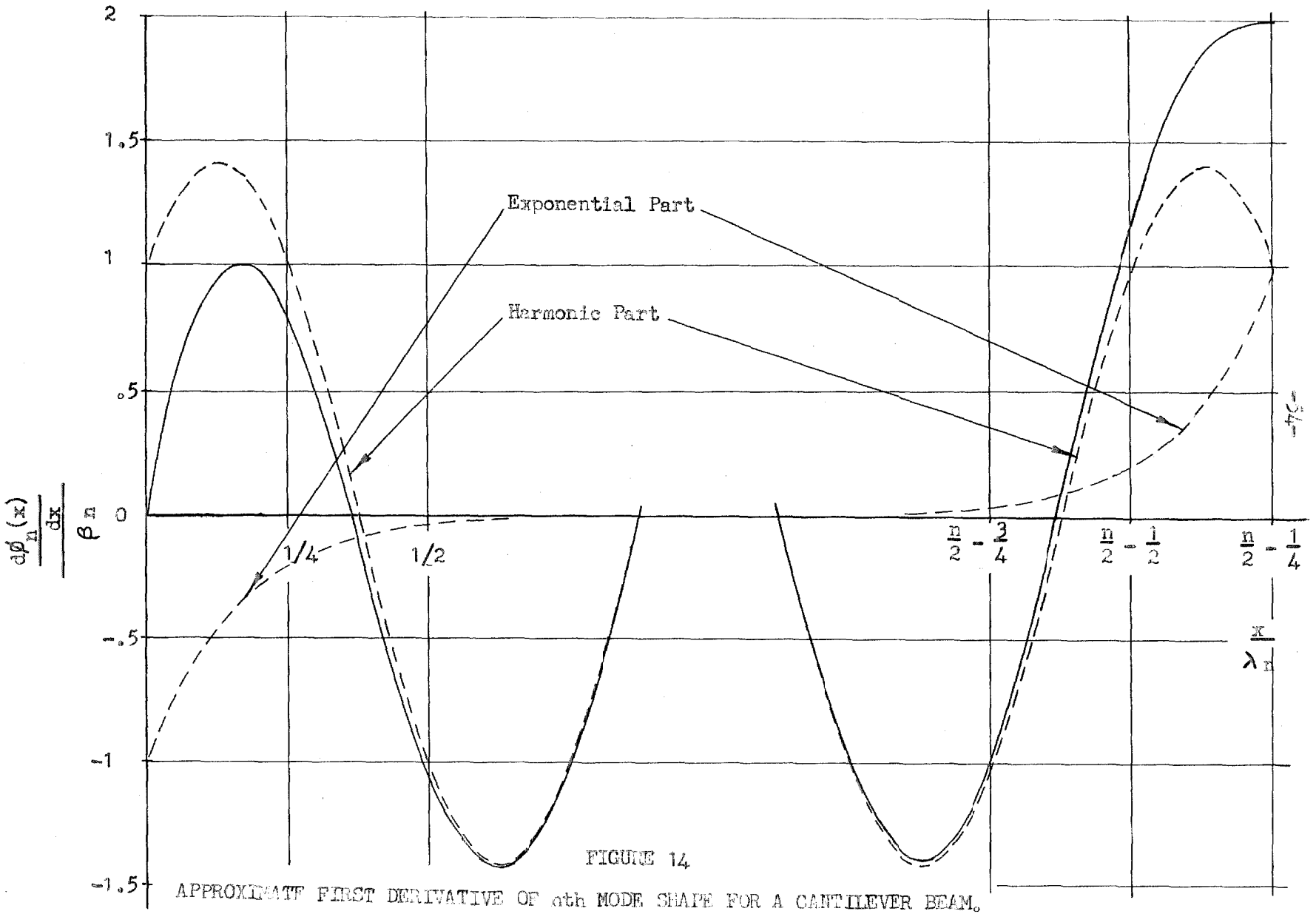

FIGURE 14

APPROXIMATE FIRST DERIVATIVE OF nth MODE SHAPE FOR A CANTILEVER BEAM.

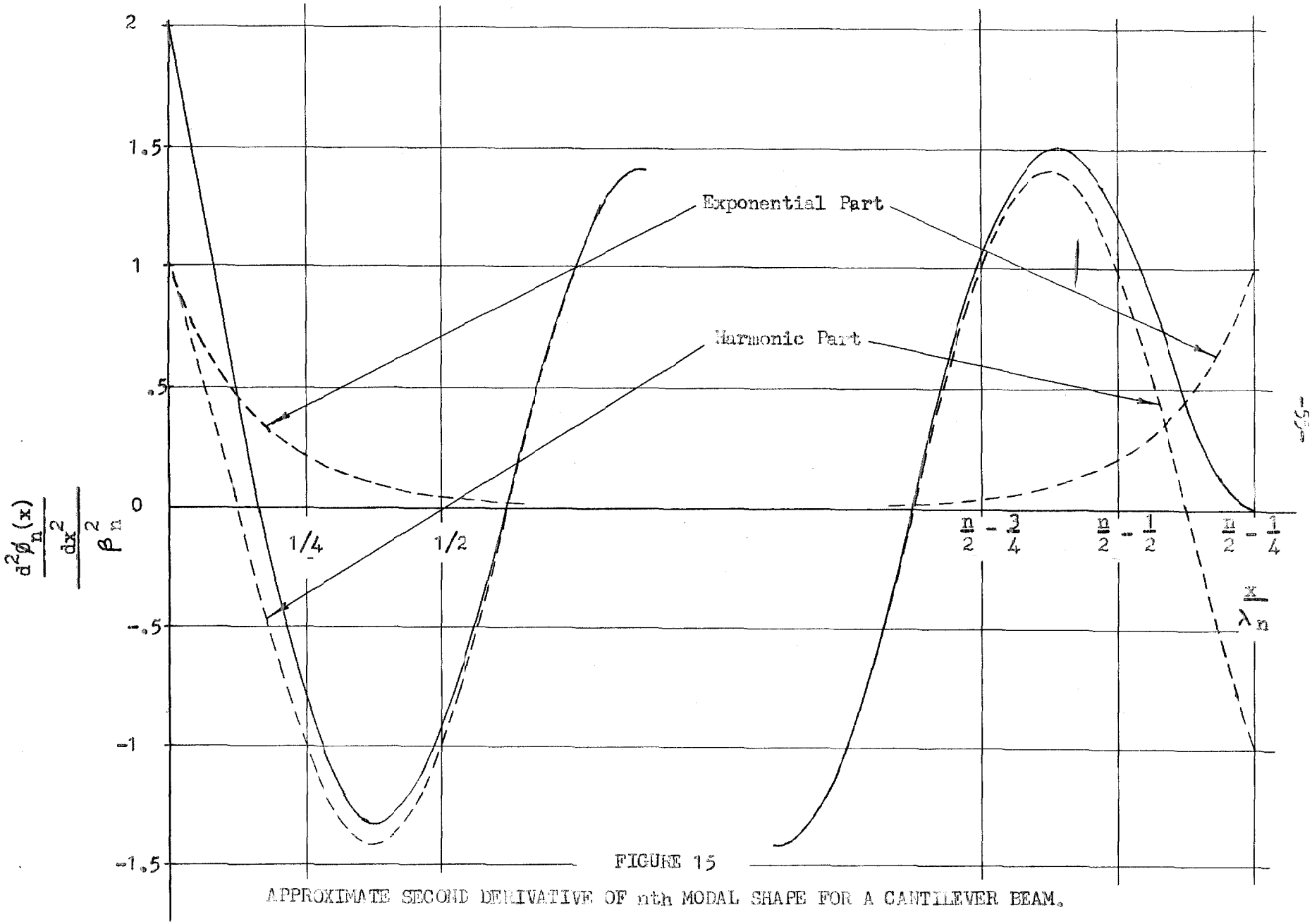

FIGURE 15

APPROXIMATE SECOND DERIVATIVE OF nth MODAL SHAPE FOR A CANTILEVER BEAM.

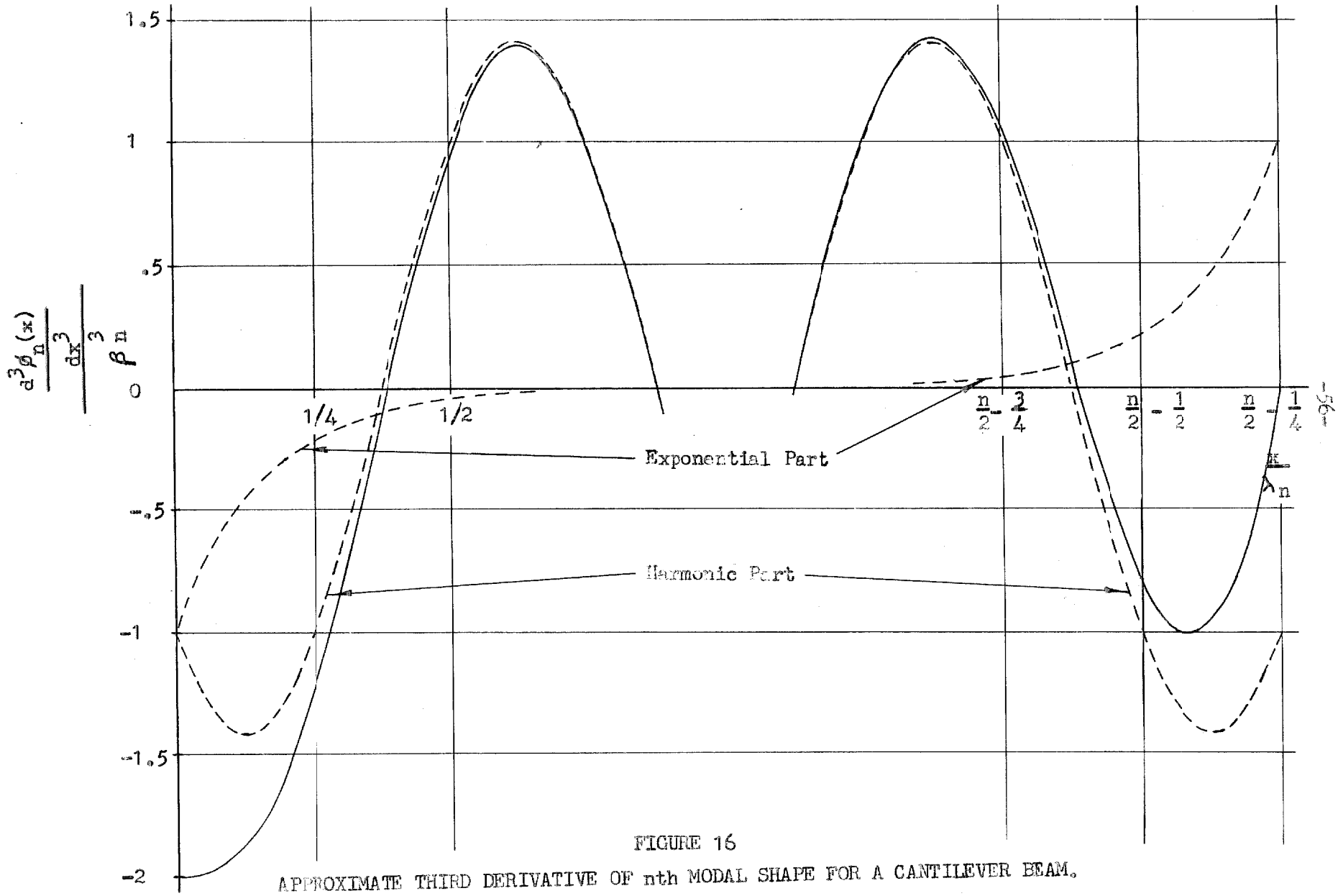

FIGURE 16

APPROXIMATE THIRD DERIVATIVE OF nth MODAL SHAPE FOR A CANTILEVER BEAM.

cantilever beam agree everywhere within 1°/o of the approximate derivatives given on Figs. 14 through 16.

Consideration of other special cases establishes that the mode shapes resulting from any boundary conditions are harmonic except near the ends of the beam. In the neighborhood of built-in or free-ends, the mode shapes and derivatives given in Figs. 13 through 16 are general for the higher modes. For example, the exact mode shapes and derivatives for the third mode of a free-free beam agree within 1°/o of the approximate values for a cantilever beam except near the built-in end. For pinned-ends, the higher mode shapes and derivatives are harmonic to the end of the beam.

Since the higher mode shapes and derivatives are harmonic except near free or built-in ends, independent of the boundary conditions, it can be established that the higher mode responses a half standing wave length or more from a boundary are independent of the boundary conditions. Assume that the harmonic part of the mode shapes is normalized to unit amplitude. The generalized forces, defined by eq. (5), depend on the force distribution relative to the mode shapes and amplitude. The generalized masses, defined by eq. (4), converge on the mass of the beam in the higher modes. The natural frequencies are, from eq. (16):

$$\omega_n = (2\pi)^2 \frac{c_1 r}{\lambda_n^2}. \qquad (57)$$

They are functions of the speed of sound in the material and the radius of gyration of the cross section relative to the standing wave length of the modes. The dynamic amplification factors are functions of the relationship between the natural frequencies and the time characteristics of the applied force.

It is evident that the response in the higher modes a half standing wave length or more from a boundary is independent of the boundary conditions. The response is a function of the apatial distribution and time characteristics of the force, the total mass of the beam, the properties of the material, the cross section, and the standing wave length. If a mode in each of two beams with different boundary conditions compare in these quantities, the response in these modes will be comparable. Even the response near a boundary is of the same order of magnitude since the mode shapes and derivatives are never more than $\sqrt{2}$ times their values elsewhere on the beam.

II. TIMOSHENKO THEORY

1. Derivation of the Equations of Motion and the Boundary Conditions.

The equations of motion considered here are those of Timoshenko (Ref. 1). Eqs. (c) and (d) of this reference were used instead of the usual eq. (139). As will be seen, this results in simplification of the boundary conditions and details of the solution. These equations, modified to include an arbitrarily distributed transverse force, are, in Timoshenko's terms:

$$EI \frac{\partial^2 \Psi}{\partial x^2} + k'AG \left(\frac{\partial y}{\partial x} - \Psi\right) - I \rho \frac{\partial^2 \Psi}{\partial t^2} = 0 \qquad (58)$$

$$\rho A \frac{\partial^2 y}{\partial t^2} - k'AG \left(\frac{\partial^2 y}{\partial x^2} - \frac{\partial \Psi}{\partial x}\right) = w(x, t). \qquad (59)$$

Ψ is the slope due to bending. The other symbols are as used in this paper. The derivation of these equations involves the statement of the equilibrium of the linear and angular, elastic and inertial forces. The equations require that the slopes and deflections be small. It is assumed that cross sections remain plane in bending. The behavior of cross

sections with respect to shear deflections is not so clear. The shear stresses are assumed to vary over the cross section which requires that they warp. However, warping cross sections lead to axial motion of the material which is not considered in the derivation. It can, perhaps, best be said that cross sections in shear are free to warp but that the resulting axial inertia forces are neglected in the derivation. The equations require that the beam be prismatic and that the force be applied in one of the principal planes.

An alternative form of eqs. (58) and (59) which will be used in this paper can be obtained by a transformation of variables to y_b and y_s, the deflection due to bending and to shear.

$$\Psi = \frac{\partial y_b}{\partial x} \tag{60}$$

$$y = y_b + y_s. \tag{61}$$

The transformation of variables, eqs. (60) and (61), yields the equations of motion:

$$EI \frac{\partial^3 y_b}{\partial x^3} + k'AG \frac{\partial y_s}{\partial x} - I\rho \frac{\partial^3 y_b}{\partial x\, \partial t^2} = 0 \tag{62}$$

$$\rho A \frac{\partial^2 y_b}{\partial t^2} + \rho A \frac{\partial^2 y_s}{\partial t^2} - k'AG \frac{\partial^2 y_s}{\partial x^2} = w(x, t). \qquad (63)$$

This form of the equations leads to particularly simple boundary conditions.

Eqs. (62) and (63) can also be derived from energy considerations utilizing Hamilton's Principle. In the process of this derivation, the boundary conditions are generated.

There has been in the literature some question as to the boundary conditions for the Timoshenko theory, particularly for built-in ends. Some of the confusion resulted from the use of the single Timoshenko equation in one variable for which the boundary conditions are not simple.

Consider an element of a beam. The kinetic and potential energies of the beam element in vibration are assumed to be:

$$d(K.E.) = \frac{1}{2} \rho A \left(\frac{\partial y_b}{\partial t} + \frac{\partial y_s}{\partial t}\right)^2 dx + \frac{1}{2} \rho I \left(\frac{\partial^2 y_b}{\partial x \, \partial t}\right)^2 dx \qquad (64)$$

$$d(P.E.) = \frac{1}{2} k'AG \left(\frac{\partial y_s}{\partial x}\right)^2 dx + \frac{1}{2} EI \left(\frac{\partial^2 y_b}{\partial x^2}\right)^2 dx. \qquad (65)$$

Included in the kinetic energy are the energies of the transverse motion and the rotational motion, the latter involving

only bending. Energy in the axial motion caused by distortion of the cross sections due to shear is neglected. Included in the potential energy are the elastic energies resulting from the shear forces and bending moments.

According to Hamilton's extended Principle for non-conservative systems, the motion of the beam must be such as to result in a stationary value of the integral

$$\int_{t_1}^{t_2} (\text{K.E.} - \text{P.E.} + W)\, dt$$

where

$$W = \int_0^1 w(x, t)\, (y_b + y_s)\, dx. \tag{66}$$

It is assumed that positive $w(x, t)$ is in the direction of positive y_b and y_s. The beam system is non-conservative only when an external force, $w(x, t)$, is applied to the beam, neglecting damping. Hamilton's extended principle requires:

$$\delta \int_{t_1}^{t_2} (\text{K.E.} - \text{P.E.} + W)\, dt = 0 \tag{67}$$

Application of the calculus of variations to eqs. (64) through (67) yields:

$$\int_{t_1}^{t_2}\int_0^l \left\{ \left[\rho A \left(\frac{\partial^2 y_s}{\partial t^2} + \frac{\partial^2 y_b}{\partial t^2} \right) - k'AG \frac{\partial^2 y_s}{\partial x^2} - w(x,t) \right] \delta y_s \right.$$

$$\left. + \left[\rho A \left(\frac{\partial^2 y_s}{\partial t^2} + \frac{\partial^2 y_b}{\partial t^2} \right) - \rho I \frac{\partial^4 y_b}{\partial x^2 \partial t^2} + EI \frac{\partial^4 y_b}{\partial x^4} - w(x,t) \right] \delta y_b \right\} dx dt$$

$$- \int_0^l \left\{ \rho A \left(\frac{\partial y_s}{\partial t} + \frac{\partial y_b}{\partial t} \right) \Big|_{t_1}^{t_2} (\delta y_s + \delta y_b) \Big|_{t_1}^{t_2} \right.$$

$$\left. + \rho I \frac{\partial^2 y_b}{\partial x \partial t} \Big|_{t_1}^{t_2} \delta \left(\frac{\partial y_b}{\partial x} \right) \Big|_{t_1}^{t_2} \right\} dx$$

$$- \int_{t_1}^{t_2} \left\{ \left[- \rho I \frac{\partial^3 y_b}{\partial x \partial t^2} + EI \frac{\partial^3 y_b}{\partial x^3} \right] \Big|_0^l \delta y_b \Big|_0^l \right.$$

$$\left. - k'AG \frac{\partial y_s}{\partial x} \Big|_0^l \delta y_s \Big|_0^l - EI \frac{\partial^2 y_b}{\partial x^2} \Big|_0^l \delta \left(\frac{\partial y_b}{\partial x} \right) \Big|_0^l \right\} dt = 0 \qquad (68)$$

The second integral in eq. (68) vanishes since variations are not permitted at the times t_1 and t_2. In order to make the third integral vanish, proper end conditions must be assumed. If the first integral vanishes, the arguments of y_b and y_s must separately vanish. This is true for the Timoshenko beam

model since there is no explicit relation involving y_b and y_s such as would result from a constraint. This yields the equations of motion:

$$EI \frac{\partial^4 y_b}{\partial x^4} + k'AG \frac{\partial^2 y_s}{\partial x^2} - I\rho \frac{\partial^4 y_b}{\partial x^2 \partial t^2} = 0 \tag{69}$$

$$\rho A \frac{\partial^2 y_b}{\partial t^2} + \rho A \frac{\partial^2 y_s}{\partial t^2} - k'AG \frac{\partial^2 y_s}{\partial x^2} = w(x, t). \tag{70}$$

Eqs. (69) and (70) are the same as eqs. (62) and (63) except that eq. (69) is the first spatial derivative of eq. (62). It is not obvious from the energy derivation that eq. (69) will integrate to eq. (62).

The following end conditions will be considered in causing the third integral of eq. (68) to vanish.

1) Pinned-end.

2) Built-in end.

3) Free-end.

For a pinned-end, the end conditions are:

$$\delta y_b + \delta y_s = 0 \tag{71}$$

$$\frac{\partial^2 y_b}{\partial x^2} = 0. \tag{72}$$

Eqs. (71) and (72) assure that there will be no transverse motion of the end and that the bending moment at the end is zero. If eq. (71) is substituted into the third integral, the argument of δy_b or δy_s is eq. (62) which vanishes everywhere. Eq. (72) causes the remaining term to vanish. Similarly, for a built-in end, the end conditions are:

$$\delta y_b + \delta y_s = 0 \tag{73}$$

$$\frac{\partial y_b}{\partial x} = 0 \, . \tag{74}$$

For a free-end, the end conditions are:

$$\frac{\partial y_s}{\partial x} = 0 \tag{75}$$

$$\frac{\partial^2 y_b}{\partial x^2} = 0. \tag{76}$$

Eqs. (75) and (76) cause the last two terms of the third integral to vanish. The coefficient of δy_b is zero since it is eq. (62) with $\frac{\partial y_s}{\partial x} = 0$.

In summary, the necessary and sufficient end conditions are:

1) Pinned-end

$$\delta y_b + \delta y_s = 0 \tag{71}$$

$$\frac{\partial^2 y_b}{dx^2} = 0 \tag{72}$$

2) Built-in end.

$$\delta y_b + \delta y_s = 0 \tag{73}$$

$$\frac{\partial y_b}{dx} = 0 \tag{74}$$

3) Free-end.

$$\frac{\partial y_s}{\partial x} = 0 \tag{75}$$

$$\frac{\partial^2 y_b}{dx^2} = 0. \tag{76}$$

In the subsequent sections, the equations of motion, eqs. (62) and (63), will be considered.

2. The General Solution by Superposition of Normal Modes.

The approach to the solution of eqs. (62) and (63) is one of synthesis utilizing the usual elements of beam vibration solution -- harmonic functions in time and harmonic and hyperbolic functions in space. This approach leads to solutions having the form of the Bernoulli-Euler solution, eqs. (8) through (13), which gives physical insight into the problem.

A more formal approach to the problem, the solution by Laplace transforms, has been made by Uflyand (Ref. 9) for the special case of a transverse step load applied at the center of a uniform pin-ended beam. Uflyand treated the usual single Timoshenko equation. However, this solution has been shown to be incorrect by Goland and Dengler (Ref. 10) because of incorrect boundary conditions which grossly simplified the solution. In turn, Goland and Dengler supplied a Laplace transform solution of the Timoshenko equation for the case of a transverse impulse in an infinite beam. This solution is difficult to evaluate except in the hypothetical case when the Young's and shear moduli are equal. The solution of the problem in a finite beam would be considerably more involved and, as far as is known, no solutions for a finite beam have been obtained.

Assume the following solutions to the homogeneous part of eqs. (62) and (63):

$$y_b = A_b e^{\beta x} e^{i\omega t} \tag{77}$$

$$y_s = A_s e^{\beta x} e^{i\omega t} . \tag{78}$$

Substitution results in the equations:

$$[(\beta l)^2 + (\frac{\omega l}{c_1})^2] A_b + \frac{k'G}{E} (\frac{l}{r})^2 A_s = 0 \tag{79}$$

$$\frac{E}{k'G} (\frac{\omega l}{c_1})^2 A_b + \left[\frac{E}{k'G} (\frac{\omega l}{c_1})^2 + (\beta l)^2\right] A_s = 0. \tag{80}$$

In order that a solution of the form of eqs. (77) and (78) may exist, the determinant of the coefficients of eqs. (79) and (80) must vanish yielding a frequency equation:

$$\omega^2 = -\frac{1}{2}\left[(\beta l)^2 \left(\frac{c_1}{l}\right)^2 (1 + \frac{k'G}{E}) - \frac{k'G}{E}\left(\frac{c_1}{l}\right)^2 (\frac{l}{r})^2\right] \pm \sqrt{\frac{1}{4}\left[(\beta l)^2 \left(\frac{c_1}{l}\right)^2 (1 + \frac{k'G}{E}) - \frac{k'G}{E}\left(\frac{c_1}{l}\right)^2 (\frac{l}{r})^2\right] - \frac{k'G}{E}\left(\frac{c_1}{l}\right)^4 (\beta l)^4} \tag{81}$$

Another equation in ω and β will be supplied when the boundary conditions are applied to the problem, permitting the solution

for the frequencies and β . At this point, it will be assumed that there are two real sets of frequencies. This is necessary for a physically plausible solution since eqs. (62) and (63) are fourth order in time. In the next Section, where the general solution is applied to the special case of beam with pinned-ends, there are found to be two sets of real frequencies. In general, two values of β^2 correspond to every value of ω^2.

The assumption of two real sets of frequencies points toward a solution of the form:

$$y_b(x, t) = \sum_{n=1}^{\infty} \phi_n^{(1)}(x)\, q_n^{(1)}(t) + \sum_{n=1}^{\infty} \phi_n^{(2)}(x)\, q_n^{(2)}(t) \quad (82)$$

$$y_s(x, t) = \sum_{n=1}^{\infty} \Psi_n^{(1)}(x)\, q_n^{(1)}(t) + \sum_{n=1}^{\infty} \Psi_n^{(2)}(x)\, q_n^{(2)}(t). \quad (83)$$

The shape functions $\phi_n^{(1)}(x)$, $\phi_n^{(2)}(x)$, $\Psi_n^{(1)}(x)$, and $\Psi_n^{(2)}(x)$ will be called the first and second sets of mode shapes for the bending and shear deflections. The time functions $q_n^{(1)}(t)$ and $q_n^{(2)}(t)$ will be called the first and second sets of generalized coordinates with the first and second sets of natural frequencies. These quantities have the form:

$$\phi_n^{(1)}(x) = A_{bn}^{(I)}\, e^{\beta_n^{(I)} x} + B_{bn}^{(I)}\, e^{-\beta_n^{(I)} x} + A_{bn}^{(II)}\, e^{\beta_n^{(II)} x} + B_{bn}^{(II)}\, e^{-\beta_n^{(II)} x} \quad (84)$$

$$\phi_n^{(2)}(x) = A_{bn}^{(III)} e^{\beta_n^{(III)} x} + B_{bn}^{(III)} e^{-\beta_n^{(III)} x} + A_{bn}^{(IV)} e^{\beta_n^{(IV)} x} + B_{bn}^{(IV)} e^{-\beta_n^{(IV)} x} \tag{85}$$

$$\psi_n^{(1)}(x) = A_{sn}^{(I)} e^{\beta_n^{(I)} x} + B_{sn}^{(I)} e^{-\beta_n^{(I)} x} + A_{sn}^{(II)} e^{\beta_n^{(II)} x} + B_{sn}^{(II)} e^{-\beta_n^{(II)} x} \tag{86}$$

$$\psi_n^{(2)}(x) = A_{sn}^{(III)} e^{\beta_n^{(III)} x} + B_{sn}^{(III)} e^{-\beta_n^{(III)} x} + A_{sn}^{(IV)} e^{\beta_n^{(IV)} x} + B_{sn}^{(IV)} e^{-\beta_n^{(IV)} x} \tag{87}$$

$$q_n^{(1)}(t) = C_n^{(1)} \sin(\omega_n^{(1)} t + \varepsilon_n^{(1)}) \tag{88}$$

$$q_n^{(2)}(t) = C_n^{(2)} \sin(\omega_n^{(2)} t + \varepsilon_n^{(2)}). \tag{89}$$

The constants of eqs. (84) through (89) are not all independent since y_b and y_s are coupled by eqs. (62) and (63). Substitution of eqs. (82) through (89) into eqs. (62) and (63) shows that the following relations exist among the constants:

$$A_{sn}^{(I)} = -\frac{E}{k'G}\left(\frac{r}{l}\right)^2\left[\left(\beta_n^{(I)}\,l\right)^2 + \left(\frac{\omega_n^{(1)}\,l}{c_1}\right)^2\right] A_{bn}^{(I)} \quad (90)$$

$$B_{sn}^{(I)} = -\frac{E}{k'G}\left(\frac{r}{l}\right)^2\left[\left(\beta_n^{(I)}\,l\right)^2 + \left(\frac{\omega_n^{(1)}\,l}{c_1}\right)^2\right] B_{bn}^{(I)} \quad (91)$$

$$A_{sn}^{(II)} = -\frac{E}{k'G}\left(\frac{r}{l}\right)^2\left[\left(\beta_n^{(II)}\,l\right)^2 + \left(\frac{\omega_n^{(1)}\,l}{c_1}\right)^2\right] A_{bn}^{(II)} \quad (92)$$

$$B_{sn}^{(II)} = -\frac{E}{k'G}\left(\frac{r}{l}\right)^2\left[\left(\beta_n^{(II)}\,l\right)^2 + \left(\frac{\omega_n^{(1)}\,l}{c_1}\right)^2\right] B_{bn}^{(II)} \quad (93)$$

$$A_{sn}^{(III)} = -\frac{E}{k'G}\left(\frac{r}{l}\right)^2\left[\left(\beta_n^{(III)}\,l\right)^2 + \left(\frac{\omega_n^{(2)}\,l}{c_1}\right)^2\right] A_{bn}^{(III)} \quad (94)$$

$$B_{sn}^{(III)} = -\frac{E}{k'G}\left(\frac{r}{l}\right)^2\left[\left(\beta_n^{(III)}\,l\right)^2 + \left(\frac{\omega_n^{(2)}\,l}{c_1}\right)^2\right] B_{bn}^{(III)} \quad (95)$$

$$A_{sn}^{(IV)} = -\frac{E}{k'G}\left(\frac{r}{l}\right)^2\left[\left(\beta_n^{(IV)}\,l\right)^2 + \left(\frac{\omega_n^{(2)}\,l}{c_1}\right)^2\right] A_{bn}^{(IV)} \quad (96)$$

$$B_{sn}^{(IV)} = -\frac{E}{k'G}\left(\frac{r}{l}\right)^2\left[\left(\beta_n^{(IV)}\,l\right)^2 + \left(\frac{\omega_n^{(2)}\,l}{c_1}\right)^2\right] B_{bn}^{(IV)}. \quad (97)$$

It will be convenient to normalize the mode shapes:

$$\int_0^1 (\phi_n^{(1)}(x) + \psi_n^{(1)}(x))^2 \, dx = 1 \tag{98}$$

$$\int_0^1 (\phi_n^{(2)}(x) + \psi_n^{(2)}(x))^2 \, dx = 1. \tag{99}$$

The normalizing condition plus the four boundary conditions specify all the constants in the mode shapes and supply an equation in ω^2 and β^2 which, with eq. (81), permits their evaluation. The determination of the four constants in the generalized coordinates from the initial conditions requires an orthogonality relation.

Derivation of an Orthogonality Condition.

In the solution of the initial value problem, it is necessary to have a relation analogous to the orthogonality condition which is useful in solutions having a single set of generalized coordinates. The form of this relation is not that of the usual classical orthogonality condition. This condition is given by eq. (3.1) of Ref. (11) in terms of the total deflection y and the bending slope ψ. With a simple transformation of coordinates, the orthogonality condition is:

$$\int_0^l \left[\rho A(y_b + y_s)_m (y_b + y_s)_n + I\rho \left(\frac{dy_b}{dx}\right)_n \left(\frac{dy_b}{dx}\right)_m \right] dx = 0$$

$$m \neq n \qquad (100)$$

The subscripts m and n refer to two separate solutions. Eq. (100) was derived in Ref. (11) from the four basic equations of motion of a beam and for the common boundary conditions — pinned, built-in, and free-ends. It will be derived in this paper from the two equations of motion, eqs. (62) and (63), since doubt was raised by Ref. (11) that this expression could be derived from fewer, higher order equations.

Consider a solution to the homogeneous part of eqs. (62) and (63).

$$y_b = y_b(x)\, e^{i\omega t} \qquad (101)$$

$$y_s = y_s(x)\, e^{i\omega t} \qquad (102)$$

Substitution of eqs. (101) and (102) results in:

$$EI \frac{d^3 y_b}{dx^3} + k'AG \frac{dy_s}{dx} + I\rho\omega^2 \frac{dy_b}{dx} = 0 \qquad (103)$$

$$\rho A \omega^2 y_b + \rho A \omega^2 y_s + k'AG \frac{\partial^2 y_s}{\partial x^2} = 0 \qquad (104)$$

Consider two solutions to eqs. (103) and (104) denoted by the subscripts m and n. Perform the following integrations by parts:

$$\int_0^1 \left(\frac{d^3y_b}{dx^3}\right)_m \left(\frac{dy_b}{dx}\right)_n dx = \left[\left(\frac{d^2y_b}{dx^2}\right)_m \left(\frac{dy_b}{dx}\right)_n - \left(\frac{dy_b}{dx}\right)_m \left(\frac{d^2y_b}{dx^2}\right)_n \right]_0^1 + \int_0^1 \left(\frac{dy_b}{dx}\right)_m \left(\frac{d^3y_b}{dx^3}\right)_n dx \tag{105}$$

$$\int_0^1 \left(\frac{d^2y_s}{dx^2}\right)_m y_{sn}\, dx = \left[\left(\frac{dy_s}{dx}\right)_m y_{sn} - y_{sm} \left(\frac{dy_s}{dx}\right)_n \right]_0^1 + \int_0^1 y_{sm} \left(\frac{d^2y_s}{dx^2}\right)_n dx \tag{106}$$

$$\int_0^1 \left(\frac{d^2y_s}{dx^2}\right)_m y_{bn}\, dx = \left[\left(\frac{dy_s}{dx}\right)_m y_{bn} \right]_0^1 - \int_0^1 \left(\frac{dy_s}{dx}\right)_m \left(\frac{dy_b}{dx}\right)_n dx \tag{107}$$

$$\int_0^1 y_{b_m} \left(\frac{d^2 y_s}{dx^2} \right)_n dx = \left[y_{b_m} \left(\frac{dy_s}{dx} \right)_n \right]_0^1$$

$$- \int_0^1 \left(\frac{dy_b}{dx} \right)_m \left(\frac{dy_s}{dx} \right)_n dx \qquad (108)$$

Multiplying eq. (105) by EI and eqs. (106) through (108) by k'AG, sum them as follows:

$$\int_0^1 \left[EI \left(\frac{d^3 y_b}{dx^3} \right)_m \left(\frac{dy_b}{dx} \right)_n + k'AG \left(\frac{d^2 y_s}{dx^2} \right)_m y_{sn} \right.$$

$$+ k'AG \left(\frac{d^2 y_s}{dx^2} \right)_m y_{bn} - k'AG \left(\frac{dy_b}{dx} \right)_m \left(\frac{dy_s}{dx} \right)_n$$

$$- EI \left(\frac{dy_b}{dx} \right)_m \left(\frac{d^3 y_b}{dx^3} \right)_n - k'AG\, y_{sm} \left(\frac{d^2 y_s}{dx^2} \right)_n \qquad (109)$$

$$\left. - k'AG\, y_{bm} \left(\frac{d^2 y_s}{dx^2} \right)_n + k'AG \left(\frac{dy_s}{dx} \right)_m \left(\frac{dy_b}{dx} \right)_n \right] dx =$$

$$EI \left[\left(\frac{d^2 y_b}{dx^2} \right)_m \left(\frac{dy_b}{dx} \right)_n - \left(\frac{dy_b}{dx} \right)_m \left(\frac{d^2 y_b}{dx^2} \right)_n \right]_0^1$$

$$+ k'AG \left[\left(\frac{dy_s}{dx} \right)_m y_{sn} - y_{sm} \left(\frac{dy_s}{dx} \right)_n \right]_0^1$$

$$+ k'AG \left[\left(\frac{dy_s}{dx} \right)_m y_{bn} - y_{bm} \left(\frac{dy_b}{dx} \right)_n \right]_0^1 .$$

The right side of this equation vanishes with the common boundary conditions — pinned, built-in, and free-ends — given by eqs. (71) through (76). Substituting values of

$\frac{d^3y_b}{dx^3}$ and $\frac{d^2y_s}{dx^2}$ from eqs. (103) and (104) into eq. (109)

and simplifying, the orthogonality condition results:

$$\int_0^1 \left[\rho A \, (y_b + y_s)_n \, (y_b + y_s)_m + I \, \rho \left(\frac{dy_b}{dx} \right)_n \left(\frac{dy_b}{dx} \right)_m \right] dx = 0$$

$$m \neq n. \qquad (100)$$

Solution of the Initial Value Problem.

Because of the form of the orthogonality condition, it will be convenient to use for the initial values the total deflection, the total velocity, the bending slope, and the bending slope velocity. The initial conditions on eqs. (82) and (83) are:

$$y(x, 0) = \sum_{n=1}^{\infty} (\phi_n^{(1)}(x) + \psi_n^{(1)}(x))\, q_n^{(1)}(0)$$

$$+ \sum_{n=1}^{\infty} (\phi_n^{(2)}(x) + \psi_n^{(2)}(x))\, q_n^{(2)}(0) \tag{110}$$

$$\left.\frac{\partial y(x, t)}{\partial t}\right|_{t=0} = \sum_{n=1}^{\infty} (\phi_n^{(1)}(x) + \psi_n^{(1)}(x)) \left.\frac{dq_n^{(1)}(t)}{dt}\right|_{t=0}$$

$$+ \sum_{n=1}^{\infty} (\phi_n^{(2)}(x) + \psi_n^{(2)}(x)) \left.\frac{dq_n^{(2)}(t)}{dt}\right|_{t=0} \tag{111}$$

$$\left.\frac{\partial y_b(x, t)}{\partial x}\right|_{t=0} = \sum_{n=1}^{\infty} \frac{d\phi_n^{(1)}(x)}{dx}\, q_n^{(1)}(0) + \sum_{n=1}^{\infty} \frac{d\phi_n^{(2)}(x)}{dx}\, q_n^{(2)}(0) \tag{112}$$

$$\left.\frac{\partial^2 y_b(x, t)}{\partial x\, \partial t}\right|_{t=0} = \sum_{n=1}^{\infty} \frac{d\phi_n^{(1)}(x)}{dx} \left.\frac{dq_n^{(1)}(t)}{dt}\right|_{t=0}$$

$$+ \sum_{n=1}^{\infty} \frac{d\phi_n^{(2)}(x)}{dx} \left.\frac{dq_n^{(2)}(t)}{dt}\right|_{t=0} \tag{113}$$

Multiply eqs. (110) and (111) by $(\phi_m^{(1)}(x) + \psi_m^{(1)}(x))$ and eqs. (112) and (113) by

$$\frac{d\phi_m^{(1)}(x)}{dx}$$

and integrate over the beam:

$$\int_0^1 y(x, 0)\,(\phi_m^{(1)}(x) + \psi_m^{(1)}(x))\,dx =$$

$$\int_0^1 \sum_{n=1}^{\infty} (\phi_n^{(1)}(x) + \psi_n^{(1)}(x))(\phi_m^{(1)}(x) + \psi_m^{(1)}(x))\, q_n^{(1)}(0)\,dx \tag{114}$$

$$+ \int_0^1 \sum_{n=1}^{\infty} (\phi_n^{(2)}(x) + \psi_n^{(2)}(x))(\phi_m^{(1)}(x) + \psi_m^{(1)}(x))\, q_n^{(2)}(0)\,dx.$$

$$\int_0^1 \left.\frac{\partial y(x, t)}{\partial t}\right|_{t=0} (\phi_m^{(1)}(x) + \psi_m^{(1)}(x))\,dx =$$

$$\int_0^1 \sum_{n=1}^{\infty} (\phi_n^{(1)}(x) + \psi_n^{(1)}(x))(\phi_m^{(1)}(x) + \psi_m^{(1)}(x)) \left.\frac{dq_n^{(2)}(t)}{dt}\right|_{t=0} dx$$

$$+ \int_0^1 \sum_{n=1}^{\infty} (\phi_n^{(2)}(x) + \psi_n^{(2)}(x))(\phi_m^{(1)}(x) + \psi_m^{(1)}(x)) \left.\frac{dq_n^{(2)}(t)}{dt}\right|_{t=0} dx \tag{115}$$

$$\int_0^1 \left.\frac{\partial y_b(x, t)}{\partial x}\right|_{t=0} \frac{d\phi_m^{(1)}(x)}{dx}\,dx = \int_0^1 \sum_{n=1}^{\infty} \frac{d\phi_n^{(1)}(x)}{dx} \frac{d\phi_m^{(1)}(x)}{dx}\, q_n^{(1)}(0)\,dx$$

$$+ \int_0^1 \sum_{n=1}^{\infty} \frac{d\phi_n^{(2)}(x)}{dx} \frac{d\phi_m^{(1)}(x)}{dx}\, q_n^{(2)}(0)\,dx \tag{116}$$

$$\int_0^1 \left.\frac{\partial^2 y_b(x,\,t)}{\partial x\,\partial t}\right|_{t=0} \frac{d\phi_m^{(1)}(x)}{dx}\,dx =$$

$$\int_0^1 \sum_{n=1}^{\infty} \frac{d\phi_n^{(1)}(x)}{dx}\,\frac{d\phi_m^{(1)}(x)}{dx}\left.\frac{dq_n^{(1)}(t)}{dt}\right|_{t=0} dx$$

$$+\int_0^1 \sum_{n=1}^{\infty} \frac{d\phi_n^{(2)}(x)}{dx}\,\frac{d\phi_m^{(1)}(x)}{dx}\left.\frac{dq_n^{(2)}(t)}{dt}\right|_{t=0} dx \qquad (117)$$

The orthogonality condition, eq. (100), applied to the solutions, eqs. (82) and (83), requires that:

$$\int_0^1 \left[\rho A\,(\phi_n^{(1)}(x) + \psi_n^{(1)}(x))\,(\phi_m^{(1)}(x) + \psi_m^{(1)}(x)) + \rho I\,\frac{d\phi_n^{(1)}(x)}{dx}\,\frac{d\phi_m^{(1)}(x)}{dx}\right] dx = 0 \qquad m \neq n \qquad (118)$$

$$\int_0^1 \left[\rho A(\phi_n^{(2)}(x) + \psi_n^{(2)}(x))\,(\phi_m^{(2)}(x) + \psi_m^{(2)}(x)) + \rho I\,\frac{d\phi_n^{(2)}(x)}{dx}\,\frac{d\phi_m^{(2)}(x)}{dx}\right] dx = 0 \qquad m \neq n \qquad (119)$$

$$\int_0^1 \left[\rho A\,(\phi_n^{(1)}(x) + \psi_n^{(1)}(x))\,(\phi_m^{(2)}(x) + \psi_m^{(2)}(x))\right.$$

$$+ \rho I \frac{d\phi_n^{(1)}(x)}{dx} \frac{d\phi_m^{(2)}(x)}{dx} \Big] dx = 0 \qquad (120)$$

all values of m and n.

Multiply eqs. (114) and (115) by ρA and eqs. (116) and (117) by ρI. Then add the first and third and the second and fourth equations:

$$\int_0^1 \Big[y(x, 0) \rho A(\phi_m^{(1)}(x) + \Psi_m^{(1)}(x)) + \frac{\partial y_b(x, t)}{\partial x}\Big|_{t=0} \rho I \frac{d\phi_m^{(1)}(x)}{dx} \Big] dx =$$

$$\int_0^1 \sum_{n=1}^{\infty} \Big[\rho A(\phi_n^{(1)}(x) + \Psi_n^{(1)}(x))(\phi_m^{(1)}(x) + \Psi_m^{(1)}(x)) + \rho I \frac{d\phi_n^{(1)}(x)}{dx} \frac{d\phi_m^{(1)}(x)}{dx}\Big] q_n^{(1)}(0)\, dx$$

$$+ \int_0^1 \sum_{n=1}^{\infty} \Big[\rho A(\phi_n^{(2)}(x) + \Psi_n^{(2)}(x))(\phi_m^{(1)}(x) + \Psi_m^{(1)}(x)) + \rho I \frac{d\phi_n^{(2)}(x)}{dx} \frac{d\phi_m^{(1)}(x)}{dx}\Big] q_n^{(2)}(0)\, dx \qquad (121)$$

$$\int_0^1 \Big[\frac{\partial y(x, t)}{\partial t}\Big|_{t=0} \rho A(\phi_m^{(1)}(x) + \Psi_m^{(1)}(x)) + \frac{\partial^2 y_b(x,t)}{\partial x\, \partial t}\Big|_{t=0} \rho I \frac{d\phi_m^{(1)}(x)}{dx}\Big] dx =$$

$$\int_0^1 \sum_{n=1}^{\infty} \Big[\rho A(\phi_n^{(1)}(x) + \psi_n^{(1)}(x))(\phi_m^{(1)}(x) + \psi_m^{(1)}(x)) + \rho I \frac{d\phi_n^{(1)}(x)}{dx} \frac{d\phi_m^{(1)}(x)}{dx} \Big] \frac{dq_n^{(1)}(t)}{dt}\Big|_{t=0} dx$$

$$+ \int_0^1 \sum_{n=1}^{\infty} \Big[\rho A(\phi_n^{(2)}(x) + \psi_n^{(2)}(x))(\phi_m^{(1)}(x) + \psi_m^{(1)}(x)) + \rho I \frac{d\phi_n^{(2)}(x)}{dx} \frac{d\phi_m^{(1)}(x)}{dx} \Big] \frac{dq_n^{(2)}(t)}{dt}\Big|_{t=0} dx \qquad (122)$$

Utilizing the orthogonality condition, eqs. (118) through (120), solve for the initial conditions of the first set of generalized coordinates from eqs. (121) and (122):

$$q_m^{(1)}(0) = \frac{\int_0^1 \Big[y(x,0) \rho A(\phi_m^{(1)}(x) + \psi_m^{(1)}(x)) + \frac{\partial y_b(x,t)}{\partial x}\Big|_{t=0} \rho I \frac{d\phi_m^{(1)}(x)}{dx} \Big] dx}{\int_0^1 \Big[\rho A(\phi_m^{(1)}(x) + \psi_m^{(1)}(x))^2 + \rho I \left(\frac{d\phi_m^{(1)}(x)}{dx} \right)^2 \Big] dx} \qquad (123)$$

$$\left.\frac{dq_m^{(1)}(t)}{dt}\right|_{t=0} = \frac{\int_0^1 \left[\left.\frac{\partial y(x,t)}{\partial t}\right|_{t=0} \rho A(\phi_m^{(1)}(x)+\Psi_m^{(1)}(x)) + \left.\frac{\partial^2 y_b(x,t)}{\partial x\, \partial t}\right|_{t=0} \rho I \frac{d\phi_m^{(1)}(x)}{dx} \right] dx}{\int_0^1 \left[\rho A(\phi_m^{(1)}(x)+\Psi_m^{(1)}(x))^2 + \rho I \left(\frac{d\phi_m^{(1)}(x)}{dx}\right)^2 \right] dx} \tag{124}$$

Similarly the initial conditions of the second set of generalized coordinates may be obtained:

$$q_m^{(2)}(0) = \frac{\int_0^1 \left[y(x,0) \rho A(\phi_m^{(2)}(x)+\Psi_m^{(2)}(x)) + \left.\frac{\partial y_b(x,t)}{\partial x}\right|_{t=0} \rho I \frac{d\phi_m^{(2)}(x)}{dx} \right] dx}{\int_0^1 \left[\rho A(\phi_m^{(2)}(x)+\Psi_m^{(2)}(x))^2 + \rho I \left(\frac{d\phi_m^{(2)}(x)}{dx}\right)^2 \right] dx} \tag{125}$$

$$\left.\frac{dq_m^{(2)}(t)}{dt}\right|_{t=0} = \frac{\int_0^1 \left[\left.\frac{\partial y(x,t)}{\partial t}\right|_{t=0} \rho A(\phi_m^{(2)}(x)+\Psi_m^{(2)}(x)) + \left.\frac{\partial^2 y_b}{\partial x \partial t}\right|_{t=0} \rho I \frac{d\phi_m^{(2)}(x)}{dx} \right] dx}{\int_0^1 \left[\rho A(\phi_m^{(2)}(x)+\Psi_m^{(2)}(x))^2 + \rho I \left(\frac{d\phi_m^{(2)}(x)}{dx}\right)^2 \right] dx} \tag{126}$$

Define the generalized masses as:

$$M_m^{(1)} = \int_0^1 \left[\rho A(\phi_m^{(1)}(x) + \Psi_m^{(1)}(x))^2 + \rho I \left(\frac{d\phi_m^{(1)}(x)}{dx}\right)^2 \right] dx \tag{127}$$

$$M_m^{(2)} = \int_0^1 \left[\rho A(\phi_m^{(2)}(x) + \psi_m^{(2)}(x))^2 + \rho I \left(\frac{d\phi_m^{(2)}(x)}{dx} \right)^2 \right] dx \tag{128}$$

The initial conditions for the two sets of coordinates are:

$$q_m^{(1)}(0) = \frac{1}{M_m^{(1)}} \int_0^1 \left[y(x, 0) \rho A(\phi_m^{(1)} + \psi_m^{(1)}(x)) + \left. \frac{\partial y_b(x, t)}{\partial x} \right|_{t=0} \rho I \frac{d\phi_m^{(1)}(x)}{dx} \right] dx \tag{129}$$

$$\left. \frac{dq_m^{(1)}(t)}{dt} \right|_{t=0} = \frac{1}{M_m^{(1)}} \int_0^1 \left[\left. \frac{\partial y(x, t)}{\partial t} \right|_{t=0} \rho A(\phi_m^{(1)}(x) + \psi_m^{(1)}(x)) + \left. \frac{\partial^2 y_b(x, t)}{\partial x \, \partial t} \right|_{t=0} \rho I \frac{d\phi_m^{(1)}(x)}{dx} \right] dx \tag{130}$$

$$q_m^{(2)}(0) = \frac{1}{M_m^{(2)}} \int_0^1 \left[y(x, 0) \rho A(\phi_m^{(2)}(x) + \psi_m^{(2)}(x)) + \left. \frac{\partial y_b(x, t)}{\partial x} \right|_{t=0} \rho I \frac{d\phi_m^{(2)}(x)}{dx} \right] dx \tag{131}$$

$$\left.\frac{dq_m^{(2)}(t)}{dt}\right|_{t=0} = \frac{1}{M_m^{(2)}} \int_0^1 \left[\left.\frac{\partial y(x,\, t)}{\partial t}\right|_{t=0} \rho A(\phi_m^{(2)}(x) + \Psi_m^{(2)}(X)) \right.$$

$$\left. + \left.\frac{\partial^2 y_b(x,\, t)}{\partial x\, \partial t}\right|_{t=0} \rho I \frac{d\phi_m^{(2)}(x)}{dx} \right] dx \qquad (132)$$

Eqs. (129) through (132) are sufficient to specify the four sets of constants $C_n^{(1)}$, $C_n^{(2)}$, $\varepsilon_n^{(1)}$, and $\varepsilon_n^{(2)}$ in the generalized coordinates, eqs. (88) and (89).

Solution for the Response to an Arbitrary Transverse Force.

From the solution for the initial value problem, it is possible to find the solution for the case of a general transverse force. Consider homogeneous initial conditions. Determine first the result of an infinitesimal period of loading. Instantaneously all the material of the beam begins in transverse motion in shear. There can be no bending deflections from a transverse force until shear strains build up resulting in internal elastic forces and moments.

The initial conditions after an infinitesimal period of loading dt are:

$$y(x,\, 0) = 0 \qquad (133)$$

$$\left.\frac{\partial y_b(x, t)}{\partial x}\right|_{t=0} = 0 \tag{134}$$

$$\left.\frac{\partial y(x, t)}{\partial t}\right|_{t=0} = \frac{w(x, t)\, dt}{\rho A} \tag{135}$$

$$\left.\frac{\partial^2 y_b(x, t)}{\partial x\, \partial t}\right|_{t=0} = 0 \tag{136}$$

From eqs. (129) through (132), the initial conditions for the two sets of generalized coordinates are:

$$q_m^{(1)}(0) = q_m^{(2)}(0) = 0 \tag{137}$$

$$\left.\frac{dq_m^{(1)}(t)}{dt}\right|_{t=0} = \frac{1}{M_m^{(1)}} \int_0^1 w(x, t)\, (\phi_m^{(1)}(x) + \psi_m^{(1)}(x))\, dx\, dt \tag{138}$$

$$\left.\frac{dq_m^{(2)}(t)}{dt}\right|_{t=0} = \frac{1}{M_m^{(2)}} \int_0^1 w(x, t)\, (\phi_m^{(2)}(x) + \psi_m^{(2)}(x))\, dx\, dt \tag{139}$$

From eqs. (137) through (139), the response in the two sets of generalized coordinates, after loading for an infinitesimal time dt, is:

$$q_m^{(1)}(t) = \frac{\sin \omega_m^{(1)} t \cdot dt}{M_m^{(1)} \omega_m^{(1)}} \int_0^1 w(x, t) \left(\phi_m^{(1)}(x) + \Psi_m^{(1)}(x)\right) dx \tag{140}$$

$$q_m^{(2)}(t) = \frac{\sin \omega_m^{(2)} t \cdot dt}{M_m^{(2)} \omega_m^{(2)}} \int_0^1 w(x, t) \left(\phi_m^{(2)}(x) + \Psi_m^{(2)}(x)\right) dx \tag{141}$$

The solutions for the generalized coordinates after a finite loading period can be obtained by superposition in the manner of the Green's function method:

$$q_m^{(1)}(t) = \frac{1}{M_m^{(1)} \omega_m^{(1)}} \int_0^t \sin \omega_m^{(1)}(t - \tau)\, d\tau \int_0^1 w(x, \tau) \left(\phi_m^{(1)}(x) + \Psi_m^{(1)}(x)\right) dx \tag{142}$$

$$q_m^{(2)}(t) = \frac{1}{M_m^{(2)} \omega_m^{(2)}} \int_0^t \sin \omega_m^{(2)}(t - \tau)\, d\tau \int_0^1 w(x, \tau) \left(\phi_m^{(2)}(x) + \Psi_m^{(2)}(x)\right) dx \tag{143}$$

Define the generalized forces and dynamic amplification factors as:

$$Q_m^{(1)}(t) = \int_0^1 w(x, t)\,(\phi_m^{(1)}(x) + \psi_m^{(1)}(x))\,dx \tag{144}$$

$$Q_m^{(2)}(t) = \int_0^1 w(x, t)\,(\phi_m^{(2)}(x) + \psi_m^{(2)}(x))\,dx \tag{145}$$

$$u_m^{(1)}(t) = \omega_m^{(1)} \int_0^t \frac{Q_m^{(1)}(\tau)}{Q_m^{(1)}{}_{max}} \cdot \sin \omega_m^{(1)}(t - \tau)\,d\tau \tag{146}$$

$$u_m^{(2)}(t) = \omega_m^{(2)} \int_0^t \frac{Q_m^{(2)}(\tau)}{Q_m^{(2)}{}_{max}} \cdot \sin \omega_m^{(2)}(t - \tau)\,d\tau \tag{147}$$

The solutions for the generalized coordinates in the general case of transverse transient loading are:

$$q_m^{(1)}(t) = \frac{Q_m^{(1)}{}_{max}}{M_m^{(1)}\,\omega_m^{(1)\,2}}\,u_m^{(1)}(t) \tag{148}$$

$$q_m^{(2)}(t) = \frac{Q_m^{(2)}{}_{max}}{M_m^{(2)}\,\omega_m^{(2)\,2}}\,u_m^{(2)}(t) \tag{149}$$

Combining eqs. (82), (83), (148) and (149), the solutions for the bending and shear deflections in the general case of

transverse transient loading are:

$$y_b(x, t) = \sum_{n=1}^{\infty} \phi_n^{(1)}(x) \cdot \frac{Q_n^{(1)}{}_{max}}{M_n^{(1)} \omega_n^{(1)\,2}} \cdot u_n^{(1)}(t) \qquad (150)$$

$$+ \sum_{n=1}^{\infty} \phi_n^{(2)}(x) \cdot \frac{Q_n^{(2)}{}_{max}}{M_n^{(2)} \omega_n^{(2)\,2}} \cdot u_n^{(2)}(t)$$

$$y_s(x, t) = \sum_{n=1}^{\infty} \Psi_n^{(1)}(x) \cdot \frac{Q_n^{(1)}{}_{max}}{M_n^{(1)} \omega_n^{(1)\,2}} \cdot u_n^{(1)}(t)$$

$$+ \sum_{n=1}^{\infty} \Psi_n^{(2)}(x) \cdot \frac{Q_n^{(2)}{}_{max}}{M_n^{(2)} \omega_n^{(2)\,2}} \cdot u_n^{(2)}(t) \qquad (151)$$

This solution shows marked similarity with the general solution for the total deflections in the Bernoulli-Euler theory, eqs. (8). The definitions of the generalized masses and forces and the dynamic amplification factors given by eqs. (127), (128) and (144) through (147) are also similar in form to those for the Bernoulli-Euler theory given by eqs. (4), (5), and (7). The solutions for the bending moment and shear force in the beam are:

$$M(x, t) = EI \left[\sum_{n=1}^{\infty} \frac{d^2\phi_n^{(1)}(x)}{dx^2} \cdot \frac{Q_n^{(1)}{}_{max}}{M_n^{(1)}\, \omega_n^{(1)\,2}} \cdot u_n^{(1)}(t) \right.$$

$$\left. + \sum_{n=1}^{\infty} \frac{d^2\phi_n^{(2)}(x)}{dx^2} \cdot \frac{Q_n^{(2)}{}_{max}}{M_n^{(2)}\, \omega_n^{(2)\,2}} \cdot u_n^{(2)}(t) \right] \qquad (152)$$

$$V(x, t) = k'AG \left[\sum_{n=1}^{\infty} \frac{d\Psi_n^{(1)}(x)}{dx} \cdot \frac{Q_n^{(1)}{}_{max}}{M_n^{(1)}\, \omega_n^{(1)\,2}} \cdot u_n^{(1)}(t) \right.$$

$$\left. + \sum_{n=1}^{\infty} \frac{d\Psi_n^{(2)}(x)}{dx} \cdot \frac{Q_n^{(2)}{}_{max}}{M_n^{(2)}\, \omega_n^{(2)\,2}} \cdot u_n^{(2)}(t) \right] \qquad (153)$$

The solution given by eqs. (150) through (153) is evidently sufficient. There are precisely the number of constants in the solution to satisfy all the initial and boundary conditions. It has been recognized (Ref. 11) that the solution of the Timoshenko equation by a single series can not be sufficient since the equations of motion are fourth order in time and there are only two sets of arbitrary constants in the single set of generalized coordinates. That criticism does not apply to the given solution.

The solution is predicated on the existence of two sets of real frequencies. The next Section reveals that there are two sets for the case of a beam with pinned-ends.

3. The Transient Response of a Pin-Ended Beam.

It is evident in this special case that the mode shapes $\phi_n^{(1)}(x)$, $\phi_n^{(2)}(x)$, $\Psi_n^{(1)}(x)$, and $\Psi_n^{(2)}(x)$ are sinusoidal with nodes at the beam ends. The consequence of this is:

$$\beta_n^{(I)}l = \beta_n^{(II)}l = \beta_n^{(III)}l = \beta_n^{(IV)}l = in\pi \tag{154}$$

Substitution of these values of β into the frequency equation, eq. (81), yields two sets of real frequencies:

$$(\omega_n^{(1)})^2 = \frac{1}{2}\left[(n\pi)^2\left(\frac{c_1}{l}\right)^2\left(1+\frac{k'G}{E}\right)+\left(\frac{c_1}{l}\right)^2\left(\frac{l}{r}\right)^2\frac{k'G}{E}\right] - \sqrt{\frac{1}{4}\left[(n\pi)^2\left(\frac{c_1}{l}\right)^2\left(1+\frac{k'G}{E}\right)+\left(\frac{c_1}{l}\right)^2\left(\frac{l}{r}\right)^2\frac{k'G}{E}\right]^2-(n\pi)^4\left(\frac{c_1}{l}\right)^4\frac{k'G}{E}} \tag{155}$$

$$(\omega_n^{(2)})^2 = \frac{1}{2}\left[(n\pi)^2\left(\frac{c_1}{l}\right)^2\left(1+\frac{k'G}{E}\right)+\left(\frac{c_1}{l}\right)^2\left(\frac{l}{r}\right)^2\frac{k'G}{E}\right] + \sqrt{\frac{1}{4}\left[(n\pi)^2\left(\frac{c_1}{l}\right)^2\left(1+\frac{k'G}{E}\right)+\left(\frac{c_1}{l}\right)^2\left(\frac{l}{r}\right)^2\frac{k'G}{E}\right]^2-(n\pi)^4\left(\frac{c_1}{l}\right)^4\frac{k'G}{E}} \tag{156}$$

Utilizing eqs. (90) through (99), the normalized mode shapes are:

$$\phi_n^{(1)}(x) = \frac{\sqrt{2}\sin\frac{n\pi x}{l}}{1 + \frac{E}{k'G}\left(\frac{r}{l}\right)^2\left[(n\pi)^2 - \left(\frac{\omega_n^{(1)}l}{c_1}\right)^2\right]} \tag{157}$$

$$\phi_n^{(2)}(x) = \frac{\sqrt{2}\sin\frac{n\pi x}{l}}{1 + \frac{E}{k'G}\left(\frac{r}{l}\right)^2\left[(n\pi)^2 - \left(\frac{\omega_n^{(2)}l}{c_1}\right)^2\right]} \tag{158}$$

$$\psi_n^{(1)}(x) = \frac{\sqrt{2}\frac{E}{k'G}\left(\frac{r}{l}\right)^2\left[(n\pi)^2 - \left(\frac{\omega_n^{(1)}l}{c_1}\right)^2\right]\sin\frac{n\pi x}{l}}{1 + \frac{E}{k'G}\left(\frac{r}{l}\right)^2\left[(n\pi)^2 - \left(\frac{\omega_n^{(1)}l}{c_1}\right)^2\right]} \tag{159}$$

$$\psi_n^{(2)}(x) = \frac{\sqrt{2}\frac{E}{k'G}\left(\frac{r}{l}\right)^2\left[(n\pi)^2 - \left(\frac{\omega_n^{(2)}l}{c_1}\right)^2\right]\sin\frac{n\pi x}{l}}{1 + \frac{E}{k'G}\left(\frac{r}{l}\right)^2\left[(n\pi)^2 - \left(\frac{\omega_n^{(2)}l}{c_1}\right)^2\right]} \tag{160}$$

An application of the defining equations, eqs. (127) and (128), yields the generalized masses:

$$M_n^{(1)} = m\left[1 + \frac{(n\pi)^2\left(\frac{r}{l}\right)^2}{\left\{1 + \frac{E}{k'G}\left(\frac{r}{l}\right)^2\left[(n\pi)^2 - \left(\frac{\omega_n^{(1)}l}{c_1}\right)^2\right]\right\}^2}\right] \tag{161}$$

$$M_n^{(2)} = m \left[1 + \frac{(n\pi)^2 \left(\frac{r}{l}\right)^2}{\left\{ 1 + \frac{E}{k'G} \left(\frac{r}{l}\right)^2 \left[(n\pi)^2 - \left(\frac{\omega_n^{(2)} l}{c_1} \right)^2 \right] \right\}^2} \right] \tag{162}$$

The generalized forces in this special case are, by eqs. (144) and (145):

$$Q_n^{(1)}(t) = Q_n^{(2)}(t) = \sqrt{2} \int_0^1 w(x, t) \sin \frac{n\pi x}{l} \, dx \tag{163}$$

The dynamic amplification factors can be obtained by eqs. (146) and (147).

The quantities in the solution, eqs. (155) through (163), are easy to evaluate and tabulate as was the case with the solution for the Bernoulli-Euler theory. The two sets of frequencies, eqs. (155) and (156), were calculated for solid rectangular and solid circular cross sections and were plotted in dimensionless form on Figs. 17 and 18 . The mode shapes and generalized masses, eqs. (157) through (162), were calculated over the same range of n $(\frac{r}{l})$ for solid rectangular and solid circular cross sections and are tabulated in dimensionless form on Figs. 19 through 21. The generalized forces and dynamic amplification factors can be determined easily by eqs. (146), (147) and (163) from the spatial and time characteristics of the applied force.

The nature of the solution can be discerned by a

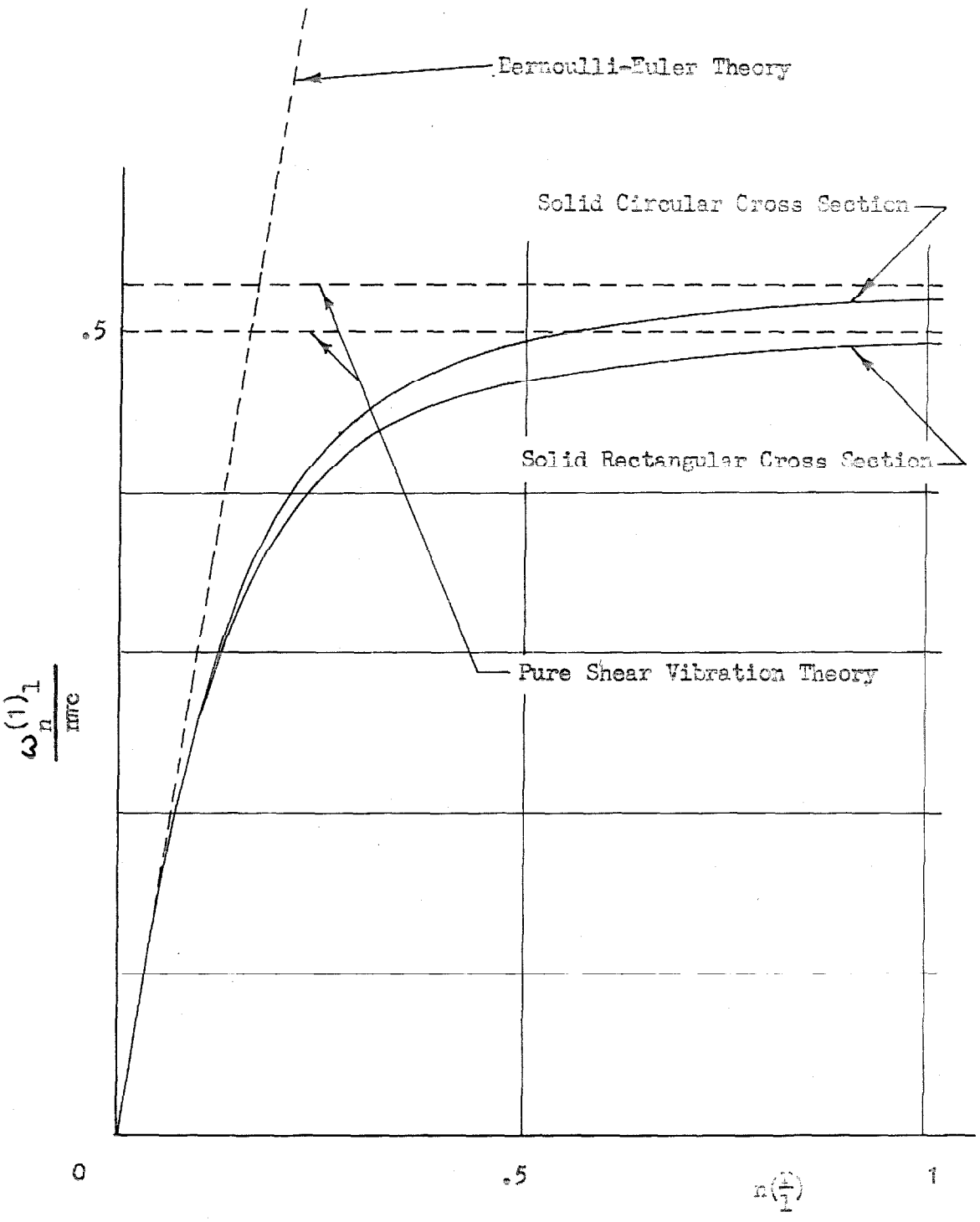

FIGURE 17

FIRST SET OF NATURAL FREQUENCIES, TIMOSHENKO THEORY, PIN-ENDED BEAM.

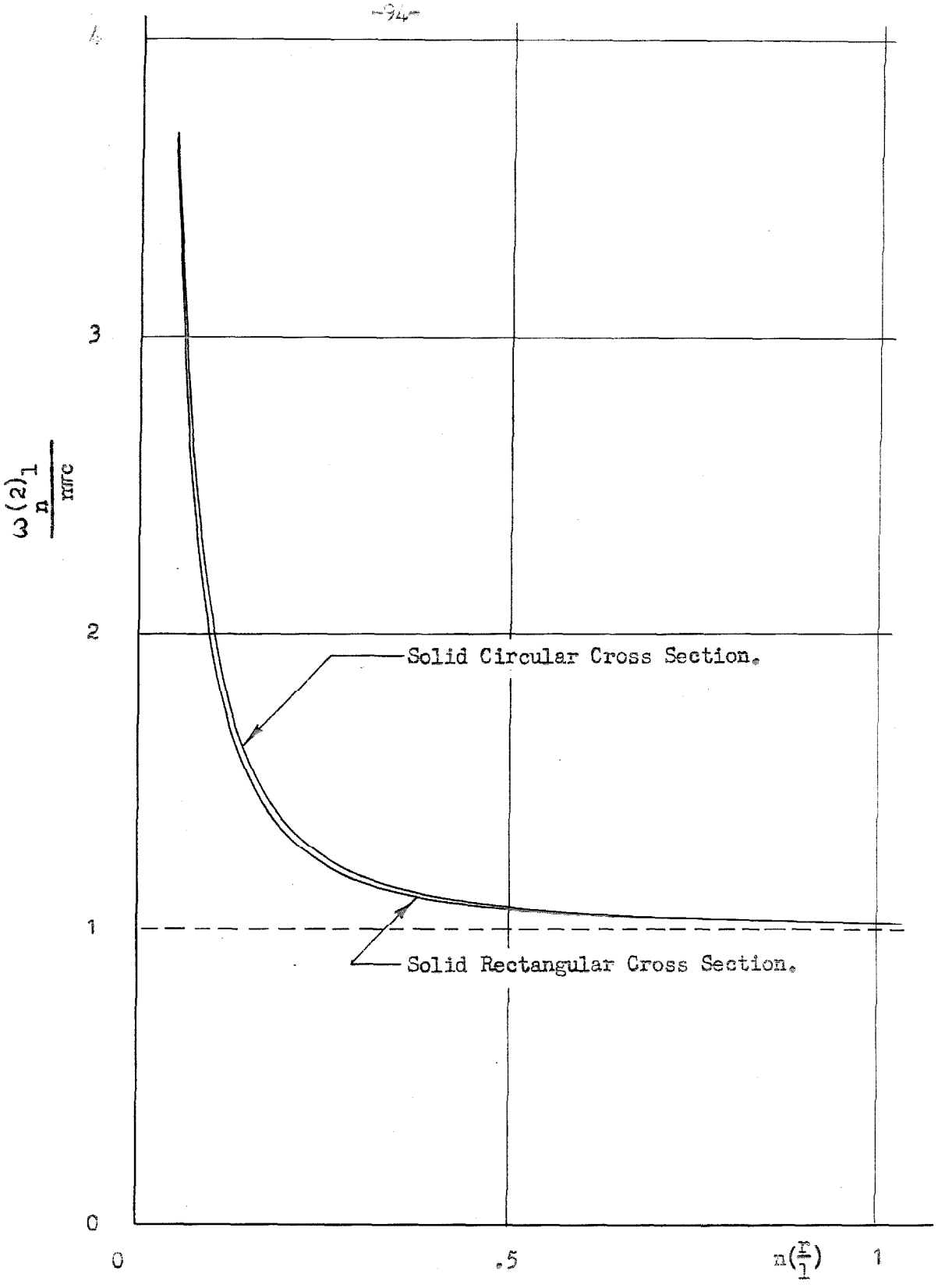

FIGURE 18

SECOND SET OF NATURAL FREQUENCIES, TIMOSHENKO THEORY, PIN-ENDED BEAM.

$n(\frac{r}{l})$	$\frac{M_n^{(1)}}{m}$ Rectangular Cross Section	$\frac{M_n^{(1)}}{m}$ Circular Cross Section	$\frac{M_n^{(2)}}{m}$ Rectangular Cross Section	$\frac{M_n^{(2)}}{m}$ Circular Cross Section
.01	1.001	1.001	1025	1022
.05	1.021	1.021	49.73	48.78
.1	1.053	1.056	19.97	18.83
.2	1.071	1.082	15.01	13.14
.3	1.059	1.072	18.06	14.97
.4	1.044	1.056	23.80	19.00
.5	1.033	1.042	31.58	24.59
1	1.010	1.014	97.93	72.66
1.5	1.005	1.007	208.9	153.2
2.5	1.002	1.002	564.4	411.0

FIGURE 19

GENERALIZED MASSES, PIN-ENDED BEAM,

TIMOSHENKO THEORY.

$n(\frac{r}{l})$	$\frac{\phi_n^{(1)}(x)}{\sin \frac{n\pi x}{l}}$	$\frac{\phi_n^{(2)}(x)}{\sin \frac{n\pi x}{l}}$	$\frac{\Psi_n^{(1)}(x)}{\sin \frac{n\pi x}{l}}$	$\frac{\Psi_n^{(2)}(x)}{\sin \frac{n\pi x}{l}}$
.01	1.409	.006	(-) 1440	1442
.05	1.290	.125	62.85	64.26
.1	1.034	.381	19.61	21.02
.2	.601	.813	8.426	9.840
.3	.363	1.051	6.198	7.612
.4	.236	1.179	5.374	6.788
.5	.163	1.251	4.979	6.393
1	.046	1.369	4.432	5.846
1.5	.021	1.393	4.327	5.742
2.5	.008	1.407	4.274	5.688

FIGURE 20

NORMALIZED MODE SHAPES, PIN-ENDED BEAM,

SOLID RECTANGULAR CROSS SECTION, TIMOSHENKO THEORY.

$n(\frac{r}{l})$	$\frac{\phi_n^{(1)}(x)}{\sin \frac{n\pi x}{l}}$	$\frac{\phi_n^{(2)}(x)}{\sin \frac{n\pi x}{l}}$	$\frac{\Psi_n^{(1)}(x)}{\sin \frac{n\pi x}{l}}$	$\frac{\Psi_n^{(2)}(x)}{\sin \frac{n\pi x}{l}}$
			(-)	
.01	1.409	.005	1439	1440
.05	1.303	.112	62.23	63.65
.1	1.066	.348	19.01	20.42
.2	.646	.768	7.842	9.257
.3	.402	1.013	5.608	7.022
.4	.265	1.149	4.775	6.189
.5	.185	1.229	4.373	5.787
1	.053	1.361	3.811	5.225
1.5	.024	1.390	3.702	5.116
2.5	.009	1.405	3.646	5.060

FIGURE 21

NORMALIZED MODE SHAPES, PIN-ENDED BEAM,

SOLID CIRCULAR CROSS SECTION, TIMOSHENKO THEORY.

scrutiny of the tabulated elements of the solution. It is suspected that the bending deflections y_b will approach the deflections predicted by the Bernoulli-Euler theory in the lower modes in slender beams. In the higher modes, it is suspected that the shear deflections y_s will approach those predicted by pure shear vibration theory. It can be shown that these suppositions are correct.

An examination of Fig. 17 reveals that the frequencies $\omega_n^{(1)}$ are asymptotic to the Bernoulli-Euler frequencies for small values of n $(\frac{r}{l})$ corresponding to the lower modes in slender beams. For larger values of n $(\frac{r}{l})$, corresponding to the higher modes, the frequencies $\omega_n^{(1)}$ are asymptotic to the frequencies of pure shear vibrations. The frequencies $\omega_n^{(2)}$ on Fig. 18 have no such physical interpretation. However, the addition of the shear mechanism of deformation may explain the existence of two frequencies since this mechanism essentially results in each mode having two degrees of freedom. While more comprehensive than the common theory, the Timoshenko theory is an inexact mathematical model and the solution may not be factual.

In order to determine the nature of the solution, the magnitude of the modewise deflection responses less the dynamic amplification factors were calculated and tabulated on Fig. 22 as functions of n $(\frac{r}{l})$ for the special case of a

$n\left(\frac{r}{l}\right)$	$\frac{\phi_n^{(1)}(x)\, Q_n^{(1)}{}_{max}}{M_n^{(1)}\, \omega_r^{(1)2}} \Big/ \frac{F \max \sin \frac{n\pi x}{l}}{m\left(\frac{n\pi c_1}{l}\right)^2}$	$\frac{\phi_n^{(2)}(x)\, Q_n^{(2)}{}_{max}}{M_n^{(2)}\, \omega_n^{(2)2}} \Big/ \frac{F \max \sin \frac{n\pi x}{l}}{m\left(\frac{n\pi c_1}{l}\right)^2}$	$\frac{\psi_n^{(1)}(x)\, Q_n^{(1)}{}_{max}}{M_n^{(1)}\, \omega_n^{(1)2}} \Big/ \frac{F \max \sin \frac{n\pi x}{l}}{m\left(\frac{n\pi c_1}{l}\right)^2}$	$\frac{\psi_n^{(2)}(x)\, Q_n^{(2)}{}_{max}}{M_n^{(2)}\, \omega_n^{(2)2}} \Big/ \frac{F \max \sin \frac{n\pi x}{l}}{m\left(\frac{n\pi c_1}{l}\right)^2}$
		(-)		
.01	2027	.01	7.99	.01
.05	81.22	.16	7.83	.16
.1	20.63	.37	7.59	.40
.2	5.522	.457	7.467	.533
.3	2.612	.361	7.557	.443
.4	1.533	.266	7.664	.337
.5	1.008	.198	7.747	.253
1	.264	.062	7.918	.082
1.5	.119	.028	7.962	.038
2.5	.020	.011	7.986	.014

FIGURE 22

MODEWISE DEFLECTION RESPONSES, PIN-ENDED BEAM, TRANSIENT TRANSVERSE FORCE AT MIDPOINT.

transverse force at the center of a pin-ended beam. It will be noted that the first set of mode responses in the bending deflection predominates for small n $(\frac{r}{l})$. For larger n $(\frac{r}{l})$, the first set of mode responses in the shear deflection predominates. For all values of n $(\frac{r}{l})$, the second set of mode responses in both bending and shear deflections are relatively small.

4. Comparison of the Bending Moment and Shear Force Responses for the Bernoulli-Euler and the Timoshenko Theories for a Special Case.

Having obtained a solution for the more comprehensive theory including the effects of shear and rotatory inertia, it is natural to compare the results to those for the more usual Bernoulli-Euler theory. The comparison will be made for the simple special case of a transverse, spatially concentrated, transient force applied at the midpoint of a pin-ended beam. For this special case, eqs. (152), (153) and (155) through (163), which yield the bending moment and shear force responses for the more comprehensive theory, can be expressed in dimensionless terms as:

$$\frac{M(x,\,t)}{l\ F\ max} = \sum_{n\,=\,1,3,5,\ldots}^{\infty} \sin\frac{n\pi x}{l}\left[A_{Mn}\,u_n^{(1)}(t) + B_{Mn}\,u_n^{(2)}(t)\right]$$

$$A_{Mn} = \sqrt{2}\left(\frac{r}{l}\right)^2 \left(\frac{\phi_n^{(1)}(x)}{\sin\frac{n\pi x}{l}}\right)\left(\frac{m}{M_n^{(1)}}\right)\left(\frac{n\pi c_1}{\omega_n^{(1)}l}\right)^2$$

$$B_{Mn} = \sqrt{2}\left(\frac{r}{l}\right)^2 \left(\frac{\phi_n^{(2)}(x)}{\sin\frac{n\pi x}{l}}\right)\left(\frac{m}{M_n^{(2)}}\right)\left(\frac{n\pi c_1}{\omega_n^{(2)}l}\right)^2 \qquad (164)$$

$$\frac{V(x,\,t)}{F\ max} = \sum_{n\,=\,1,3,5,\ldots}^{\infty} \cos\frac{n\pi x}{l}\left[A_{Vn}\,u_n^{(1)}(t) + B_{Vn}\,u_n^{(2)}(t)\right]$$

$$A_{Vn} = \sqrt{2}\,\frac{k'G}{E}\;\frac{1}{n\pi}\left(\frac{\psi_n^{(1)}(x)}{\sin\frac{n\pi x}{l}}\right)\left(\frac{m}{M_n^{(1)}}\right)\left(\frac{n\pi c_1}{\omega_n^{(1)}l}\right)^2$$

$$B_{Vn} = \sqrt{2}\,\frac{k'G}{E}\;\frac{1}{n\pi}\left(\frac{\psi_n^{(2)}(x)}{\sin\frac{n\pi x}{l}}\right)\left(\frac{m}{M_n^{(2)}}\right)\left(\frac{n\pi c_1}{\omega_n^{(2)}l}\right)^2 \tag{165}$$

Also for this special case, eqs. (9) and (10), the solutions for the bending moment and shear force responses from the Bernoulli-Euler theory, become, in dimensionless terms:

$$\frac{M(x,\,t)}{l\ F\ max} = \sum_{n\,=\,1,3,5,\ldots}^{\infty} \sin\frac{n\pi x}{l}\;C_{Mn}\,u_n(t) \tag{166}$$

$$C_{Mn} = \frac{2}{(n\pi)^2}$$

$$\frac{V(x,\,t)}{F\ max} = \sum_{n\,=\,1,3,5,\ldots}^{\infty} \cos\frac{n\pi x}{l}\,C_{Vn}\,u_n(t) \tag{167}$$

$$C_{Vn} = \frac{2}{n\pi}$$

The coefficients A_{Mn}, B_{Mn}, A_{Vn}, and B_{Vn} are all functions of the slenderness ratio l/r, the ratio of Young 's modulus to shear modulus E/G, the shape of the cross section, and the mode number. A slenderness ratio of $l/r = 20$ was arbitrarily chosen for this special case. A solid rectangular cross section

was assumed. The ratio of Young's to shear modulus E/G was selected as 8/3 which closely approximates the properties of steel. With the aid of Figs. 17 through 20, the coefficients were evaluated for a number of modes and tabulated on Figs. 23 and 24 as the percent of C_{M1} and C_{V1} respectively.

A study of Fig. 23 for the bending moment coefficients reveals the B_{Mn} is substantially smaller than A_{Mn}. In the lower modes B_{Mn} is relatively negligible while in the higher modes B_{Mn} approaches, as a relative maximum, 1/4 of A_{Mn}. It can be seen that $A_{Mn} + B_{Mn} = C_{Mn}$. This fact can also be deduced from eqs. (164) through (167). In the case where the force is applied statically, the two solutions must be equal. Since the dynamic amplification factors are all unity in this case and, since there can be only one unique expansion of the static bending moment in a sine series, the above equality must be true. The coefficients C_{Mn} accordingly approach A_{Mn} very closely in the lower modes and approach, as a relative minimum, in the higher modes, 3/4 of A_{Mn}.

A similar study of Fig. 24 for the shear force coefficients shows that B_{Vn} is substantially smaller than A_{Vn}. In the higher modes particularly, B_{Vn} becomes relatively insignificant. As in the case of the bending moment response, $A_{Vn} + B_{Vn} = C_{Vn}$.

The results clearly show that, in the bending moment

n	A_{Mn}	B_{Mn}	C_{Mn}
		(-)	
1	100.19	.19	100
3	11.68	.57	11.11
5	4.509	.509	4
7	2.424	.383	2.041
9	1.517	.282	1.235
11	1.038	.211	.827
21	.2966	.0699	.2267
31	.1375	.0334	.1041
51	.0511	.0126	.0385

(Expressed as percent of first mode Bernoulli-Euler response).

FIGURE 23

MODEWISE BENDING MOMENT RESPONSE COEFFICIENTS, PIN-ENDED BEAM, TRANSIENT TRANSVERSE FORCE AT MIDPOINT.

n	A_{Vn}	B_{Vn}	C_{Vn}
1	98.39	1.61	100
3	31.17	2.16	33.33
5	18.76	1.24	20
7	13.59	.70	14.29
9	10.71	.40	11.11
11	8.840	.251	9.091
21	4.717	.045	4.762
31	3.211	.015	3.226
51	1.957	.004	1.961

(Expressed as percent of first mode Bernoulli-Euler response).

FIGURE 24

MODEWISE SHEAR FORCE RESPONSE COEFFICIENTS, PIN-ENDED BEAM,

TRANSIENT TRANSVERSE FORCE AT MIDPOINT.

and shear force responses from the more comprehensive theory, the response in the first set of frequencies predominates. It is further apparent that the bending moment and shear force responses in the Bernoulli-Euler theory are modewise comparable to those of the more comprehensive theory. These conclusions however are dependent also on the magnitude of the dynamic amplification factors.

In order to consider the additional effects of the dynamic amplification factors, it will be necessary to study a specific force -- time transient. Consider the case of a half-sine-wave-in-time transient force. In this case it will be convenient to refer to Fig. 6 for the dynamic amplification factors. If the force is applied slowly enough to excite statically all the modes, the bending moment and shear force responses in the two theories will be modewise identical. This will also be true for all those higher modes that are essentially statically excited even when the lower modes are dynamically excited.

If the force is applied rapidly enough that ωt_1 is less than π for some of the modes, these modes will be impulsively excited. Consider the case of impulsive excitation of all the modes. In this limiting case, it is not convenient to use eqs. (164) through (167). For the case of a pure impulse, eqs. (164) through (167) become:

$$\frac{M(x,\,t)}{c_1\ \mathrm{Imp}} = \sum_{n\,=\,1,3,5,\ldots}^{\infty} \left(\frac{r}{l}\right)^2 (n\pi)\left(\frac{\phi_n^{(1)}(x)}{\sin\frac{n\pi x}{l}}\right)\left(\frac{m}{M_n^{(1)}}\right)$$

$$\cdot\left(\frac{n\pi c_1}{\omega_n^{(1)}{}_1}\right)\sin\frac{n\pi x}{l}\,\sin\omega_n^{(1)}t + \sum_{n\,=\,1,3,5,\ldots}^{\infty}\left(\frac{r}{l}\right)^2 (n\pi)\left(\frac{\phi_n^{(2)}(x)}{\sin\frac{n\pi x}{l}}\right)$$

$$\cdot\left(\frac{m}{M_n^{(2)}}\right)\left(\frac{n\pi c_1}{\omega_n^{(2)}{}_1}\right)\sin\frac{n\pi x}{l}\,\sin\omega_n^{(2)}t \qquad (168)$$

$$\frac{V(x,\,t)\,l}{c_1\ \mathrm{Imp}} = \sum_{n\,=\,1,3,5,\ldots}^{\infty}\left(\frac{k'G}{E}\right)\left(\frac{\Psi_n^{(1)}(x)}{\sin\frac{n\pi x}{l}}\right)\left(\frac{m}{M_n^{(1)}}\right)\left(\frac{n\pi c_1}{\omega_n^{(1)}{}_1}\right)$$

$$\cdot\cos\frac{n\pi x}{l}\,\sin\omega_n^{(1)}t + \sum_{n\,=\,1,3,5,\ldots}^{\infty}\left(\frac{k'G}{E}\right)\left(\frac{\Psi_n^{(2)}(x)}{\sin\frac{n\pi x}{l}}\right)$$

$$\cdot\left(\frac{m}{M_n^{(2)}}\right)\left(\frac{n\pi c_1}{\omega_n^{(2)}{}_1}\right)\cos\frac{n\pi x}{l}\,\sin\omega_n^{(2)}t \qquad (169)$$

$$\frac{M(x,\,t)}{c_1\ \mathrm{Imp}} = 2\left(\frac{r}{l}\right)\sum_{n\,=\,1,3,5,\ldots}^{\infty}\sin\frac{n\pi x}{l}\,\sin\omega_n t \qquad (170)$$

$$\frac{V(x,\,t)\,l}{c_1\ \mathrm{Imp}} = 2\left(\frac{r}{l}\right)\sum_{n\,=\,1,3,5,\ldots}^{\infty}(n\pi)\cos\frac{n\pi x}{l}\,\sin\omega_n t \qquad (171)$$

The bending moment and shear force responses, eqs. (168) through (171), were determined for a number of modes and were tabulated on Figs. 25 and 26 as the percent of the first mode bending moment and shear force responses in the Bernoulli-Euler theory. An examination of Figs. 25 and 26 shows that the modewise bending moment and shear force responses in the two theories become progressively divergent in the higher modes. This is due to the divergence of the frequencies in the two theories in the higher modes. When modes are impulsively excited, the dynamic amplification factors vary linearly as the natural frequencies. A divergence of frequencies would thus result in a divergence of dynamic amplification factors and of mode responses.

In the usual case of transient excitation, the lower modes are dynamically excited while the higher modes are essentially statically excited. Consider the special case when $\omega_1^{(1)} t_1 = \pi/10$. For this case, the maximum bending moment and shear force responses given by eqs. (164) through (167) were determined for a number of modes for the periods $0 \leq \frac{t}{t_1} \leq 1$ and $1 \leq \frac{t}{t_1}$. The responses are tabulated on Figs. 27 through 30 as the percent of the maximum first mode bending moment and shear force responses from the Bernoulli-Euler theory for the period $1 \leq \frac{t}{t_1}$. In comparing the responses in the Bernoulli-Euler theory to those of the first set of frequencies in

	Timoshenko	Bernoulli-Euler	
n	first set of modes	second set of modes	
1	94.62	4.17	100
3	74.10	16.36	100
5	58.86	19.79	100
7	48.15	19.14	100
9	40.35	17.40	100
11	34.52	15.57	100
21	19.53	9.48	100
31	13.47	6.64	100
51	8.27	4.12	100

(Expressed as percent of maximum first mode Bernoulli-Euler response).

FIGURE 25

MAXIMUM MODEWISE BENDING MOMENT RESPONSES, PIN-ENDED BEAM, TRANSVERSE IMPULSE AT MIDPOINT.

	Timoshenko	Bernoulli-Euler	
n	first set of modes	second set of modes	
1	92.92	43.15	100
3	197.78	62.09	300
5	244.81	48.20	500
7	270.05	34.57	700
9	284.84	24.97	900
11	294.02	18.53	1100
21	310.66	6.04	2100
31	314.69	2.88	3100
51	316.94	1.09	5100

(Expressed as percent of maximum first mode Bernoulli-Euler response).

FIGURE 26

MAXIMUM MODEWISE SHEAR FORCE RESPONSES, PIN-ENDED BEAM, TRANSVERSE IMPULSE AT MIDPOINT.

	Timoshenko	Bernoulli-Euler	
n	first set of modes	second set of modes	
1	14.80	1.54	16.56
3	58.06	4.01	82.42
5	37.32	3.01	30.08
7	19.66	2.03	10.73
9	11.11	1.57	6.40
11	6.75	1.14	4.15
21	1.64	.35	1.10
31	.72	.16	.50
51	.25	.06	.18

(Expressed as percent of maximum first mode Bernoulli-Euler response, $\frac{t}{t_1} \geq 1$).

FIGURE 27

MAXIMUM MODEWISE BENDING MOMENT RESPONSES, $0 \leq \frac{t}{t_1} \leq 1$, PIN-ENDED BEAM, TRANSVERSE HALF SINE WAVE FORCE AT MIDPOINT, $\omega_1^{(1)} t_1 = \frac{\pi}{10}$.

	Timoshenko		Bernoulli-Euler
n	first set of modes	second set of modes	
1	94.61	.91	100
3	66.75	1.37	80.58
5	36.60	1.23	8.78
7	13.90	.31	1.13
9	1.65	.28	.85
11	2.22	.25	.18
21	.017	.039	.021
31	.105	.001	.009
51	.006	.003	.001

(Expressed as percent of maximum first mode Bernoulli-Euler response, $\frac{t}{t_1} \geq 1$).

FIGURE 28

MAXIMUM MODEWISE BENDING MOMENT RESPONSES, $\frac{t}{t_1} \geq 1$, PIN-ENDED BEAM, TRANSVERSE HALF SINE WAVE FORCE AT MIDPOINT, $\omega_1^{(1)} t_1 = \frac{\pi}{10}$.

	Timoshenko	Bernoulli-Euler	
n	first set of modes	second set of modes	
1	14.54	15.97	16.56
3	155.0	15.2	247.3
5	155.2	7.3	150.4
7	110.3	3.7	75.06
9	78.33	2.25	57.36
11	57.51	1.35	45.70
21	26.07	.23	23.04
31	16.77	.07	15.42
51	9.71	.02	9.32

(Expressed as percent of maximum first mode Bernoulli-Euler response, $\frac{t}{t_1} \geq 1$).

FIGURE 29

MAXIMUM MODEWISE SHEAR FORCE RESPONSES, $0 \leq \frac{t}{t_1} \leq 1$, PIN-ENDED BEAM, TRANSVERSE HALF SINE WAVE FORCE AT MIDPOINT, $\omega_1^{(1)} t_1 = \frac{\pi}{10}$.

	Timoshenko	Bernoulli-Euler	
n	first set of modes	second set of modes	
1	92.96	9.46	100
3	178.2	5.2	241.7
5	152.31	3.00	43.91
7	77.99	.57	7.90
9	11.67	.40	7.67
11	18.90	.30	1.96
21	.28	.02	.44
31	2.46	-	.28
51	.24	-	.04

(Expressed as percent of maximum first mode Bernoulli-Euler response, $\frac{t}{t_1} \geq 1$)

FIGURE 30

MAXIMUM MODEWISE SHEAR FORCE RESPONSES, $\frac{t}{t_1} \geq 1$, PIN-ENDED BEAM, TRANSVERSE HALF SINE WAVE FORCE AT MIDPOINT, $\omega_1^{(1)} t_1 = \frac{\pi}{10}$.

the more comprehensive theory, a significant trend can be observed. The response in the first few modes in the Bernoulli-Euler theory predominates over the response in the more comprehensive theory while in the subsequent modes the reverse is true. As in the purely impulsive case, this trend is due to the divergence of the frequencies predicted by the two theories. Since the natural frequencies predicted by the Bernoulli-Euler theory increase more rapidly with n than those of the lower set of frequencies in the more comprehensive theory, the impulsively excited modes will be exaggerated by the Bernoulli-Euler theory. For the same reason, the non-impulsively excited modes will approach static excitation more rapidly with the mode number in the Bernoulli-Euler theory and therefore be underestimated.

Since the mode shapes are sinusoidal in both theories for the pin-ended beam, the generalized forces will vary in the same manner in the two theories for any spatial distribution of forces. Relatively, then the responses in the two theories for any spatial distribution of forces are the same as given here for a single spatially concentrated force at the midpoint.

In general, it can be concluded that the response in the more comprehensive theory for a pin-ended beam is predominantly in the lower set of frequencies. Further, it can be concluded that the modal bending moment and shear

force responses in this predominant set of frequencies is of the same order of magnitude as those of the Bernoulli-Euler theory, provided the dynamic amplification factors are comparable. The Bernoulli-Euler theory overestimates the dynamic amplification factors for the impulsively excited modes and underestimates them for the non-impulsively excited modes. These conclusions are true for any spatial distribution of force.

CONCLUSIONS

I. Bernoulli-Euler Theory

An advantage of the mode superposition solution given in Section 1 is the ease with which the quantities in the solution can be tabulated for a number of situations in a concise form. Available in the literature are tabulations of the mode shapes or characteristic functions, their first three derivatives, and the characteristic numbers for the six common beams for the first five modes. For use in considering the beam response to a particular, simple transient force, a graph of dynamic amplification factors for the case of a half sine wave transient force is presented in Section 2 in a more comprehensive form than given in the literature.

The convergence of the terms or modes in the solution is of importance since it is convenient to calculate only a few of the modes in any case. The subject of mode convergence is considered in a general way in Section 3. It is concluded that the convergence becomes poorer as the impressed transient force is concentrated spatially and in time. The manner in which the modal bending moment and shear force responses converge or diverge with the mode number as the transient force is concentrated spatially and in time is indicated in Section 3. It is demonstrated that the mode convergence is poorer for an applied bending moment than for an applied force.

It is believed in some quarters that the dynamic response in an elastic structure to a rapidly or suddenly applied force is never larger than twice the expected static response. It is concluded in Section 4 that the dynamic response at each point in a beam to such a force can be greater than twice the expected static response at the same point. The conclusion is true whether the force is distributed or concentrated. Dynamic responses larger than twice the static responses were commented on by Frankland (Ref. 7).

It is demonstrated in Section 5 that the mode responses in the higher modes are essentially independent of the boundary conditions except within one-half wave length of free or clamped boundaries. This fact permits the extension of conclusions based on a beam with particular end conditions to beams with other end conditions. It is shown that the mode shapes and their derivatives are harmonic with an exponential transition which is significant only within one-half wave length of free or clamped boundaries. With the aid of the figures of Section 5, the higher mode shapes and derivatives can be sketched accurately for the common end conditions.

II. Timoshenko Theory

In considering the effects of shear deflections and rotatory inertia on the flexural vibrations of beams, the Timoshenko equations of motion are used. Instead of the usual single equation in one variable, two equations of motion in two variables are treated.

As a result, the boundary conditions are simplified and the solutions for the elastic bending moment and shear force are simplified. In Section 1, the equations of motion are derived from Hamilton's principle. In the process of the derivation, the end conditions for free, clamped, and pinned ends are generated.

Presented in Section 2 is a new, general, mode superposition solution of the Timoshenko equations of motion. The solution is in the form of two infinite series involving two sets of generalized coordinates and two sets of mode shapes. The existence of this solution requires the existence of two sets of frequencies. The solution appears to be sufficient and completely specified by the boundary and initial conditions. The quantities in the solution are analogous to those for the solution of the Bernoulli-Euler equation except that there are two sets instead of one.

In Section 3, it is shown that there are two sets of frequencies in the case of a pin-ended beam. The quantities in the solution for a pin-ended beam are tabulated as functions of the parameter $n(\frac{r}{l})$ for solid rectangular and solid circular cross sections. The deflection solution approaches that of the Bernoulli-Euler equation in magnitude and frequency for the lower modes of long, slender beams. In the higher modes, the deflection solution approaches that for pure shear vibrations in magnitude and frequency. The response in the first set of frequencies predominates.

In Section 4, a comparison between the bending moment and

shear force solutions of the Timoshenko and Bernoulli-Euler equations is made for a pin-ended beam subjected to a concentrated transient force at the midpoint. A slenderness ration $l/r = 20$ and a solid rectangular cross section are selected. It is concluded that the bending moment and shear force responses in the predominant set of frequencies are of the same order of magnitude modewise as those in the Bernoulli-Euler solution provided that the dynamic amplification factors are comparable. The Bernoulli-Euler solution overestimates the dynamic amplification factors for the impulsively excited modes and underestimates them for the non-impulsively excited modes. It appears that the Bernoulli-Euler solution will give good results for the bending moment and shear force solutions if the predominant set of frequencies of the Timoshenko solution is used to calculate the dynamic amplification factors.

NOMENCLATURE

$y(x, t)$	=	total transverse deflection.
$y_b(x, t)$	=	transverse bending deflections.
$y_s(x, t)$	=	transverse shear deflections.
x	=	index of position along the beam axis.
t	=	time.
$M(x, t)$	=	elastic bending moment in the beam.
$V(x, t)$	=	elastic shear force in the beam.
$w(x, t)$	=	arbitrary distributed transverse force.
$F(t)$	=	arbitrary concentrated transverse force.
$M_A(t)$	=	arbitrary concentrated applied bending moment.
Imp	=	concentrated transverse impulse.
t_1	=	half period of half sine wave transient force.
E	=	Young's modulus.
G	=	shear modulus.
k'	=	ratio of average shear stress to maximum shear stress over a cross section.
l	=	length of beam.
r	=	radius of gyration of cross section around the principal axis normal to the plane of motion.
λ	=	standing wave length of a mode of vibration.
c_1	=	speed of a dilatational elastic wave in the material.

I = moment of inertia of cross section around the principal axis normal to the plane of motion.

A = cross section area.

ρ = mass density of the material.

m = mass of beam.

c = coefficient of viscous damping.

c_c = critical viscous damping.

$DLF(x)$ = dynamic load factor.

K.E. = kinetic energy.

P.E. = potential energy.

Bernoulli-Euler Theory:

$\phi_n(x)$ = nth mode shape or characteristic function.

$q_n(t)$ = nth generalized coordinate.

M_n = nth generalized mass.

$Q_n(t)$ = nth generalized force.

ω_n = nth natural frequency.

$\beta_n l$ = nth characteristic number.

$u_n(t)$ = nth dynamic amplification factor.

Timoshenko Theory:

$\phi_n(x)$ = nth mode shape in the bending deflection.

$\Psi_n(x)$ = nth mode shape in the shear deflection.

Otherwise, the same quantities as used in Bernoulli-Euler Theory, except with superscripts 1 and 2 to indicate two sets.

A, B, C, and ε with subscripts and superscripts are used as constants. In each instance, they are defined in the text.

REFERENCES

1. Timoshenko, S.P., Vibration Problems in Engineering, (1947) Second Edition, D. Van Nostrand Co. Inc., Chap. VI, p. 307.

2. Biot, M.A. and Bisplinghoff, R.L., Dynamic Loads on Airplane Structures During Landing, NACA Wartime Report W92, (Oct. 1944).

3. Bisplinghoff, R.L. et al., J. Aeronaut. Sci. (May 1950) V. 17, No. 5, p. 259.

4. Williams, D., Displacements of a Linear Elastic System Under a Given Transient Load, presented at the Sixth International Congress of Applied Mechanics, (Sept. 1946), Paris, France.

5. Young, D. and Felgar, R.P., Jr., Tables of Characteristic Functions Representing Normal Modes of Vibration of a Beam, (July 1949), Univ. of Texas Publ. No. 4913.

6. Love, A.E.H., A Treatise on the Mathematical Theory of Elasticity, (1944), Fourth Edition, Dover Publ. Art. 128.

7. Frankland, J.M., Proc. Soc. of Exp. Stress Anal.,(1949), V. VI, No. 2, p. 7.

8. Mindlin, R.D. et al., Proc. Soc. of Exp. Stress Anal., (1949), V. V, No. 2, p. 69.

8a. Williams, D., Rapid Estimates of the Higher Natural Frequencies and Modes of Beams and Hence of the Stresses Induced by Transient and Periodic Loads, Reissner Anniversary Volume, (1949), J. W. Edwards, pp. 152-162.

REFERENCES

9. Uflyand, Ya. S., Akad. Nauk. SSSR Prikl. Mat. Mekli., (1948), V. 12, p. 287 (See Review 33, AMR 3).

10. Goland, M. and Dengler, M.A., Proc. of the First Nat. Congress of Applied Mech. (1951).

11. Dolph, C.L., Normal Modes of Oscillation in Beams, Report UMM 79 (1951), Willow Run Research Center, Univ. of Michigan.